2-9-2010

The formation of carbon nanofibers and thin films from the catalytic decomposition of ethylene by palladium

Mark A. Atwater

Mark Andrew Atwater
Candidate

Mechanical Engineering
Department

This thesis is approved, and it is acceptable in quality and form for publication:

Approved by the Thesis Committee:

Boyd Chad Paserman, Chairperson

Claudia C. Luhrs

Jonathan Phillips

THE FORMATION OF CARBON NANOFIBERS AND THIN FILMS FROM THE CATALYTIC DECOMPOSITION OF ETHYLENE BY PALLADIUM

BY
MARK ANDREW ATWATER

A.A.S. Toolmaking Tech., Pennsylvania College of Technology, 2007

A.A.S. Automated Mfg. Tech., Pennsylvania College of Technology, 2007

B.S.Mfg.E.Tech., Pennsylvania College of Technology, 2007

THESIS

Submitted in Partial Fulfillment of the
Requirements for the Degree of

Master of Science
Mechanical Engineering

The University of New Mexico
Albuquerque, New Mexico

December, 2009

I would like to dedicate this work to my wife, Cammie, who has continually supported me through my various efforts to further my education.

Acknowledgements

I gratefully acknowledge the support and inspiration of my advisor, Dr. Zayd Leseman. He was instrumental in bringing this work to fruition, and guiding the process to a fruitful outcome. He has been crucial in providing me with a secure and composed work environment so that I could focus on both academics and research. I would also like to thank Dr. Jonathan Phillips, of Los Alamos National Lab, for his experience, and direction during this work. Without his previous work in this area and proposition of continuing it, this project would not have existed. I am also thankful for the assistance of Dr. Claudia Luhrs, who was always very helpful in the laboratory and in teaching me characterization intricacies, as well as assisting in conceptual approaches to this research. I would also like to acknowledge the help I've received from other faculty members in conversation or otherwise, especially that of Dr. Yu-Lin Shen and Dr. Marwan Al-Haik.

In addition, I would also like to acknowledge the support I've received from the staff in the Mechanical Engineering Department. Without their support my academic and research endeavors would surely have presented much greater challenges. Also, I am indebted to David Woods for his consistent support in the machine shop and valuable insights into designing and creating equipment used in the process of this study. I would also like to thank my fellow students for their friendship and assistance with class work and research.

Outside of my support at UNM, I must acknowledge the support of my family who has continually supported me during my various pursuits, especially my parents and siblings who have been an essential and constant backing through much more than my academic career. Also, I would like to specifically thank Leonard and Cindy Gerber for their gracious assistance and the impact it has had on my academic career. I am also deeply grateful to Dorian and Dianna Atwater, who made me feel welcome and well-cared for after moving a great distance to come to Albuquerque. Finally, I thank my wife, Cammie, who has been a great inspiration and faithful companion, and has believed in me even more than myself.

The accomplishment of the completion of this program has not been an isolated effort, and I wish to grant recognition to all that have supported me throughout my pursuit, without whom, none of this would be possible.

THE FORMATION OF CARBON NANOFIBERS AND THIN FILMS FROM THE CATALYTIC DECOMPOSITION OF ETHYLENE BY PALLADIUM

BY

MARK ANDREW ATWATER

ABSTRACT OF THESIS

Submitted in Partial Fulfillment of the
Requirements for the Degree of

Master of Science
Mechanical Engineering

The University of New Mexico
Albuquerque, New Mexico

December, 2009

The Formation of Carbon Nanofibers and Thin Films from the Catalytic Decomposition of Ethylene by Palladium

by

Mark Andrew Atwater

A.A.S. Toolmaking Technology, Pennsylvania College of Technology, 2007
A.A.S. Automated Manufacturing Technology, Pennsylvania College of Technology, 2007
B.S. Manufacturing Engineering Technology, Pennsylvania College of Technology, 2007
M.S. Mechanical Engineering, University of New Mexico, 2009

ABSTRACT

It has been demonstrated that palladium can be an exceptional catalyst toward the deposition of solid carbon from ethylene in two distinct forms: nanofibers and thin films. Four forms of palladium were tested: sputtered film, foil, sub-micron powder, and nanopowder. The deposition of carbon can be achieved by a very simple method. In this method ethylene and oxygen or hydrogen are flowed through a single-zone, horizontal tube furnace at atmospheric pressure and temperatures typically from 550-700°C. The addition of a secondary gas such as oxygen or hydrogen is vital in driving the deposition. Although both gases improve deposition, the manner in which they do differs. Ethylene-oxygen mixtures are preferred at lower temperatures (i.e. 550°C) than ethylene-hydrogen mixtures (i.e. 700°C). Pd sub-micron was the most prolific form of palladium at producing solid carbon in a combustion environment, whereas nanopowder was in ethylene-hydrogen mixtures. Palladium, of any form, did not catalyze appreciable carbon deposition at any temperature in ethylene alone. These findings suggest that radical species may be imperative to inciting carbon deposition. Independent of the previous finding, it is suggested different mechanisms of growth exist for fibers and thin films. This difference in mechanism is attributed to carbon acting to self-catalyze further deposition.

The resulting carbon deposition rate and morphology were found to be a function of temperature, position in the reactor, duration of the reaction, gaseous environment, and form of palladium. These factors were all interconnected, and had to be considered collectively to predict the efficacy of the reaction toward solid carbon production. Crystallinity was found to increase with temperature, and ethylene-hydrogen mixtures produced more crystalline structures than were formed in a combustion environment, however the carbon produced under any conditions tested here was never fully graphitic, and instead was turbostratic or nearly amorphous.

Based on the findings of the general catalysis study, the promise of application for the carbon nanofibers was anticipated and demonstrated through the formation of fibrous carbon foams. These foams can be generated using a small quantity of palladium (<5% carbon output by mass), and both the macro- and microscale properties will define the overall properties, and therefore the projected use. These fibrous carbon foams can be combined with other materials to form composites which can be integrated during the formation of the foam. Because the foam process does not require high temperatures, a variety of materials with low melting temperatures can be safely incorporated. Also discussed is the potential of carbon nanofibers as an improved method of polymer reinforcement by tailoring morphology through reaction parameters.

Table of Contents

Table of Figures

1 Introduction

The advancement of science and technology has provided many benefits which are now taken for granted. As scientific discovery aids in the design of new technologies, those technologies subsequently provide assistance in furthering scientific knowledge. As this cycle gains momentum, we have experienced an outpouring of new ideas and inventions which has become expected rather than extraordinary. At the forefront of our desire for progression is the promise of smaller, more efficient, and more powerful devices by which to improve our lives. Provision of such requests has come, in part, from micro and nanoscale technologies which make such innovation attainable. Nanotechnology has been publicized as the next "industrial revolution,"[1] but to this point has not produced many of the developments expected. It is because of the wealth of possibilities still offered by the study of nanoscale structures, and their potential for incorporation into both new and existing devices, that it continues to be an attractive field of research.

Perhaps the most researched nanomaterial is the carbon nanotube (CNT). Ever since the discovery of multi-walled carbon nanotubes (MWCNTs)[2] and subsequently, single-walled carbon nanotubes (SWCNTs)[3,4] they have been intensely studied. This is because their exceptional properties and potential applications[5] are of great interest to researchers and industry. Carbon nanofibers (also called filaments) are also gaining attention. These, unlike CNTs, are solid instead of tubular, and their properties are not quite as impressive as carbon nanotubes. However, they are still attractive because, in comparison to carbon nanotubes, they are relatively simple and cheap to produce while still offering the benefit of nanoscale properties similar to those of carbon nanotubes.[6] In addition to carbon nanofibers, thin films of carbon have also been found to form, which may have applications similar to those of graphene,[7] but again, the properties are expected to be inferior, but with much simpler synthesis.

Carbon nanofibers are typically formed via the decomposition of a carbon containing gas over a catalytic metal. Palladium was chosen in this study because it is a known to be good catalyst.[8] Ethylene was chosen as the carbon feedstock because it is relatively cheap and routinely used in catalytic carbon deposition reactions.[9-16] The task of investigating the palladium-catalyzed formation of carbon nanofibers and thin films was undertaken in order to elucidate the effect of several factors on the final morphology of the deposited carbon. The factors studied herein focus on the role of temperature, gaseous environment, position in reactor (residence time), and catalyst form. All of these aspects of the reaction were found to have a dramatic impact on the result characteristics of the deposited carbon.

The first variable of interest was temperature. Carbon deposition generally occurred at temperatures between 450-700°C, but temperatures both greater and less than these were studied as well. The ideal growth* temperature varied for each form of palladium. The range of temperatures over which any appreciable growth occurred was found to be form dependent as well.

The second variable of interest is the gaseous environment. Reactions were done at atmospheric pressure, and the carbon feedstock was always ethylene (C_2H_4), but it was combined with oxygen (O_2) and hydrogen (H_2) in various ratios to investigate the effect on both carbon growth rate and growth type (i.e. morphology). The presence of secondary gases played a vital role in improving crystallinity of the deposited carbon, longevity of the catalyst, as well as the vigor of catalyst toward solid carbon deposition.

The third variable was position in the reactor. This has two important implications. The first is the temperature, which varied across the furnace in a Gaussian fashion, being highest in the center and lowering toward the inlet and outlet (detail is provided in Section 3.2.1). The second implication is the time the gas(es) have been in the furnace (residence time) which can greatly effect homogeneous reaction products (radicals) in the

* Throughout this thesis the terms growth, deposition, and formation will be used interchangeably to signify the presence of carbon after a reaction.

case of gas mixtures. It was found that growth was not merely a function of temperature, but also of position within the reactor.

The last consideration, catalyst form, was perhaps the most important in dictating the resulting carbon yield and morphology. Because all catalysts considered in this work are high purity Pd, catalyst form dictates the surface area to volume ratio (i.e. the particle or grain size). This ratio directly governs the availability of carbon species for deposition as the carbon will typically diffuse through the catalyst in order to form the fiber of the film. The catalyst forms tested were foil, sputtered film, and powder. Catalytic carbon deposition is rarely studied on such a variety of templates, and it was found that consideration of such characteristics is of the utmost importance in realizing the behavior of such metals in their various forms.

With such a broad range of considerations, illuminating the various mechanisms of growth and gaining better control of the resulting products was anticipated. However, one truth rang clear throughout this work: The mechanisms are not only complicated, but are also not presently well-understood, especially in the case of carbon thin films. The growth of carbon nanofibers has been well-documented, and although a model for creation based on a carbon adsorption, diffusion, and precipitation (ADP) model[17-21] has been widely accepted, there is still some confusion as to the role of secondary gases and radical species in generating these nanostructures. For carbon thin films, which typically encapsulate the underlying metal, the ADP model cannot be confidently applied. The ability of the carbon feedstock to reach the catalytic surface is unlikely, and this is crucial for the ADP model. A mechanism by which the encapsulating carbon layer may catalyze further carbon deposition is suggested and supported by observations made in this work and previous work by others.

The importance of carbon nanostructures in the technology of the future is undeniable. Carbon nanofibers generated by the catalytic deposition on hydrocarbons at atmospheric pressure and relatively low temperatures (< 700°C) provides a simple and inexpensive means to produce useful products in a shorter time frame than some more exotic

materials which are not yet mature enough for industrial scalability. Understanding the science is vital to quickly and effectively create new technology, and that was the continual motivation behind this work.

2 Subject Review

Carbon nanofibers, or filaments, are not at all a new area of interest. In 1889 Hughes and Chambers filed a patent for the manufacture of carbon filaments by "…the destructive distillation of a gaseous carbon compound capable of yielding carbon when decomposed by heat…"[22] This is the very process used for the majority of catalytic carbon depositions, and the basis of the work conducted herein. The characterization technology did not exist in 1889 to thoroughly study these filaments, and as that technology has advanced, so have both the understanding of, and the interest in, carbon nanofibers (CNFs).

It was not until the late 1960s and early 1970s that significant research of the properties and structure of formation was being conducted.[23-25] In 1972, Baker et al., introduced a mechanism for fiber growth[17] in which carbonaceous gas is liberated of all but the carbon atoms as a result of catalytic "cracking," and the adsorbed carbon atoms are then thermodynamically driven to deposit on the side opposite the catalytic cracking process. Tibbets et al.[21] suggest that the diffusion process is concentration driven instead of heat driven. This conclusion in supported by others,[26] but a combination of thermodynamic and concentration effects has also been proposed.[20] In general, the agreed process involves adsorption of carbon atoms followed by their diffusion into the catalyst, and subsequent precipitation elsewhere on the material. The simplified ADP model shown in Figure 1 depicts the general process by which fiber formation occurs using ethylene as the carbon feedstock. The process consists of:

A. A carbon-containing gas is supplied to the catalyst surface.
B. The gas dissociates on the surface leaving adsorbed carbon.
C. Species other than carbon desorb from the surface.
D. The carbon species then diffuse into the catalyst with a higher concentration at the gas/catalyst interface causing a concentration driven migration of carbon.
E. The carbon is precipitated as a solid fiber.

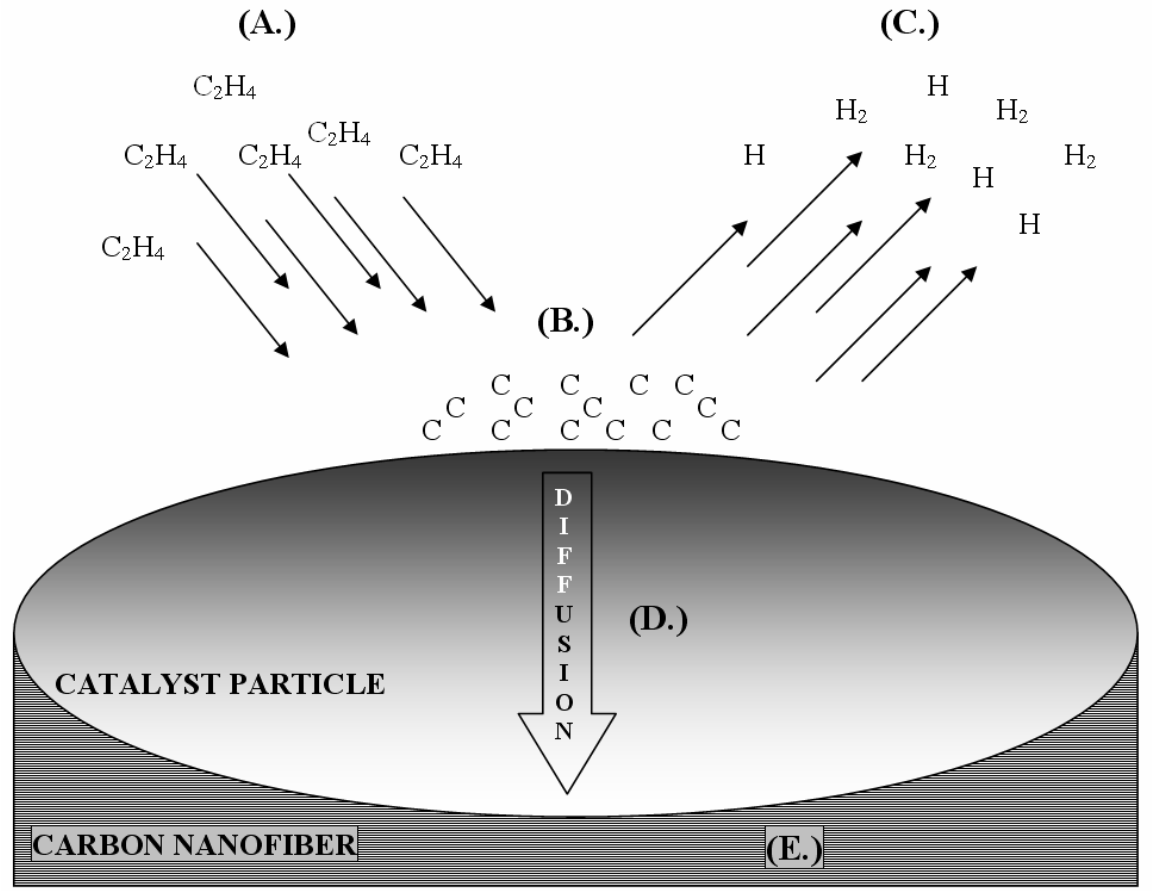

Figure 1 – Simplified Adsorption Diffusion and Precipitation (ADP) Model

The above method assumes a concentration driven diffusion process rather than by a temperature gradient. The process aside from the diffusion mechanism remains the same for both. It should also be noted that the carbon need not be isolated atoms, but instead can occur as clusters of carbon atoms. These C_n species (where *n* indicates the number of adjoined carbon atoms) are more stable than individual atoms, and too many combining together can form islands and eventually interconnect, covering the surface, poisoning the catalyst, and inhibiting further growth.[15]

The growth of fibers can occur in two key ways. The first involves a catalyst particle being supported at the end of a growing fiber, and the second has the catalyst particle in the center two coaxial fibers. These two situations are shown in Figure 2. There are other ways in which fiber growth occurs (e.g. >2 fibers from on a particle, helical/spiral growth, etc.), but these two are the simplest and most common.

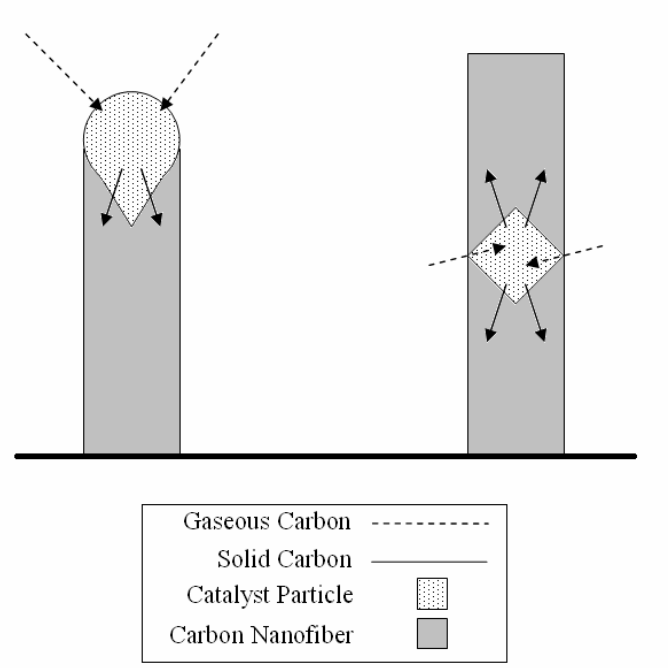

Figure 2 - Principal manners in which carbon nanofibers grow.

The process is commonly done at, or near, ambient pressure. Temperatures are typically between 500 and 1000°C, with 600-700°C being the most common. Gases are usually small hydrocarbons (e.g. methane, ethylene, etc.) or carbon monoxide (CO), and the catalytic material is usually iron or nickel. Of course there are exceptions to all of these generalizations, and indeed, the process can be done with a wide variety of gases, metals and temperatures. It is the proper combination of these factors that determines the efficiency of the process.

Most prior work focuses on the use of nickel and iron catalysts,[13,17,19,27-32] although other metals and alloys have been studied.[11,14,15,33] Palladium is rarely employed as a catalyst for solid carbon deposition and typically involves Pd precursors or non-atmospheric pressures.[34-38] This is likely due to the inefficiency of using palladium as a catalyst for carbon deposition via the thermal decomposition of hydrocarbons alone. Growth on palladium has been achieved in a pure acetylene environment resulting in a "stacked cup" morphology,[39] but acetylene is an unstable gas requiring extreme care in handling. Uniquely, the present work shows that in the correct environment carbon deposition on

palladium catalysts can be rapid at low temperature (e.g. 550°C), using mixtures of ethylene and oxygen or hydrogen.

Virtually all reported methods for producing carbon nanofibers are based on the thermal decomposition of carbon monoxide, pure hydrocarbon, or hydrocarbons mixed with hydrogen.[13,29,30] In this study, the use of ethylene, ethylene-oxygen (combustion), and ethylene-hydrogen environments are investigated for catalytic carbon deposition. In particular, it is demonstrated that growth is faster and occurs over a broader range in a combustion mixture than in pure ethylene or ethylene mixed with hydrogen.

Also investigated, is the importance of the initial form of the metal catalyst on the final product. This is a consideration not commonly made in literature. Most processes involve particles or foils only. Particles are typically produced by precipitation of a metal or metals on a substrate from a liquid medium,[12-14] or by evaporation and annealing.[39] The growth rate and type of structure proved to be dramatically impacted by the morphology of the palladium catalyst, proving to be a crucial consideration. Also typically neglected in studies is the effect of residence time, or position in reactor, on the deposition characteristics. This too proved to be important in determining the rate and morphology of carbon.

With so many ways to create carbon nanofibers, it is not surprising that they are still not well understood; even given the fact they have been, at least loosely speaking, known of since the late 19th century. Because of the versatility in producing these nanostructures, it provides much room for discovery and improvement. The more precisely the growth can be controlled, the more tunable the properties become, and then incorporation into new technologies becomes a reality.

3 Experimental Setup and Procedure

Carbon deposition was achieved using a general procedure of hydrocarbon decomposition over a palladium catalyst. The reaction was conducted at ambient pressure and optimal temperatures were between 550-700°C. Ethylene was used for the carbon feedstock in all cases, and was used in pure form, as well as mixed with oxygen or hydrogen to affect deposition characteristics such as rate and crystallinity. The reactions are comprised of two distinct themes. The first is a general deposition process to gather basic information on kinetics and morphology, whereas the second is directed specifically at using carbon nanofibers in applications such as composites and for forming fibrous carbon foams consisting entirely of carbon nanofibers.

3.1 Materials

Three forms of Pd were used in this study: sputtered film, foil, and powder. Sputtered films were deposited onto oxidized single crystal Si (100). After oxidation a thin layer of Cr (ca. 100 Å) was deposited for increased adhesion of the Pd film to the SiO_2. A thicker layer (ca. 500Å) of Pd was sputtered on to this Cr layer. Sputtered film samples were diced into squares approximately 1cm on a side before use. Pd foil (99.9%, 0.25mm thick) was purchased from Alfa Aesar and used without modification. Pd nanopowder (<25nm, 99.9%) and sub-micron powder (< 1μm, 99.9%) were both purchased from Sigma Aldrich, and also used without modification. Pd foil and film samples were cleaned with methanol purchased from Burdick Jackson (HPLC grade) before being placed in the furnace. Samples were placed on ceramic boats, also cleaned using methanol.

To help establish the crystallinity relative to known forms of carbon, pyrolyzed sucrose, graphite flakes (Alfa Aesar, 99%), graphite platelet nanofibers (Aldrich, 99%), multi wall carbon nanotubes (CheapTubes.com, >95wt%) and single wall carbon nanotubes

(CheapTubes.com, >90wt%) were also analyzed. No modifications were made before analysis.

3.2 Apparatus and Procedure

The carbon deposition was conducted in two general ways. The first, and more general of the two, was used to gather universal data on growth rate and morphology. The second was specifically designed for investigating the formation of carbon foam consisting entirely of carbon nanofibers. The apparatus is sectioned based on these two classes of experiments.

3.2.1 General Purpose Reactor

The atmospheric pressure chemical vapor deposition (APCVD) reactor consists of a 50mm diameter single zone furnace in which a 50mm diameter quartz tube resides. As shown in Figure 3, the samples were placed at regular intervals in the furnace's 30.5cm heated zone. For studies of the effects of residence time, six equally spaced samples were used per run along the heated zone.

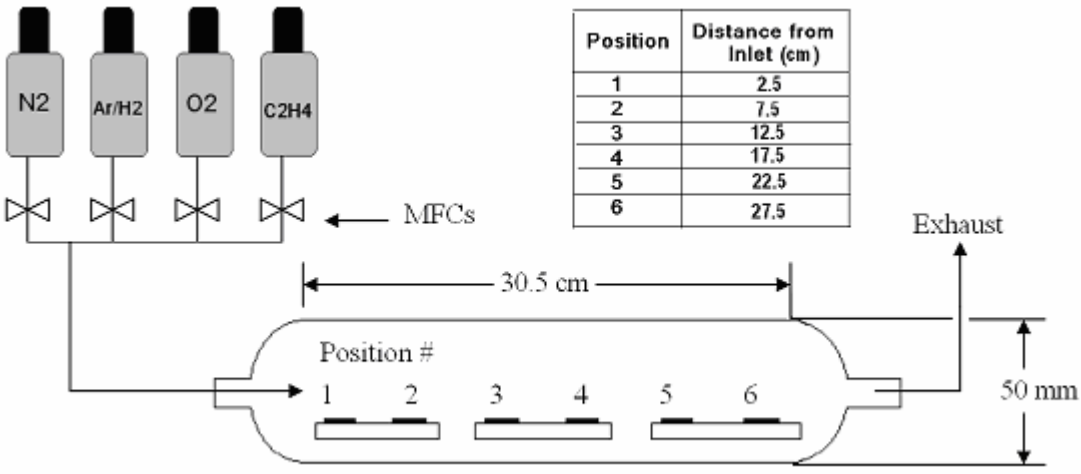

Figure 3 - APCVD reactor used for general studies of carbon deposition

The temperature varied from the inlet to outlet, as shown in Figure 4. The temperature distribution was mapped by moving a 70cm long thermocouple fitted with a ceramic sleeve down the axis of the tube and taking temperature measurements every 25mm. N_2 was flowing at 600sccm in the tube during the measurements. For the experiments that were designed to yield insight regarding the influence of residence time on both kinetics and nature of carbon growth it was important to map temperature distribution in the reactor.

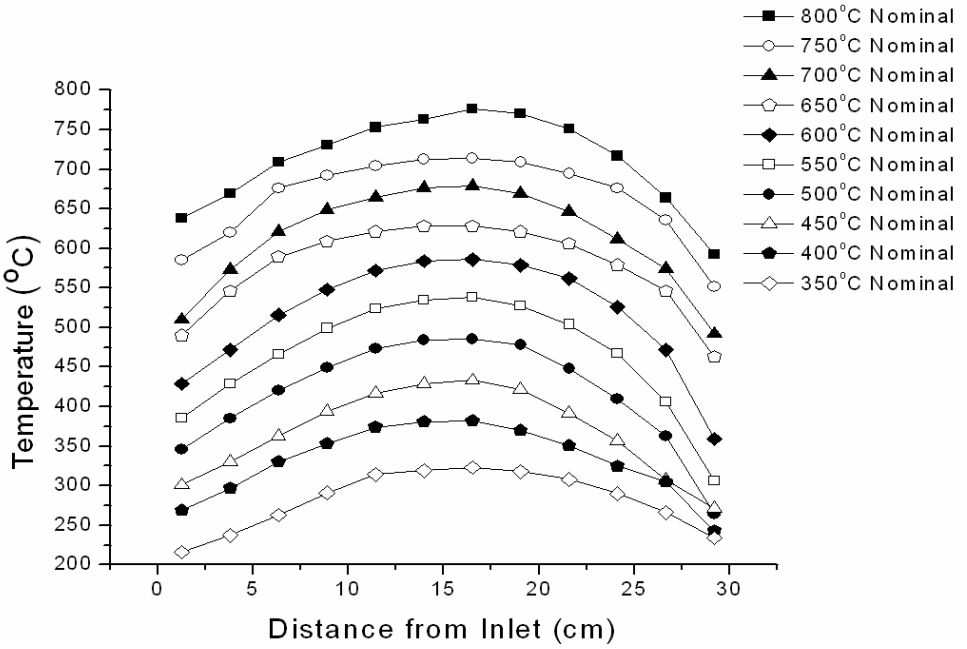

Figure 4 - Temperature distribution in furnace with 600sccm N_2 flowing

Since an exothermic reaction was expected, a higher confidence in the actual temperature of the sample surface during reaction conditions was desired. To track the influence of the reaction on sample temperature, the temperature of Pd foil was directly measured with a thermocouple, while under typical reaction conditions. As shown in Figure 5, the effect of the reaction was found to change the temperature by a maximum of 5°C. This change of temperature and the variation of temperature with position suggest the temperatures reported herein can be regarded as accurate to ± 10°C.

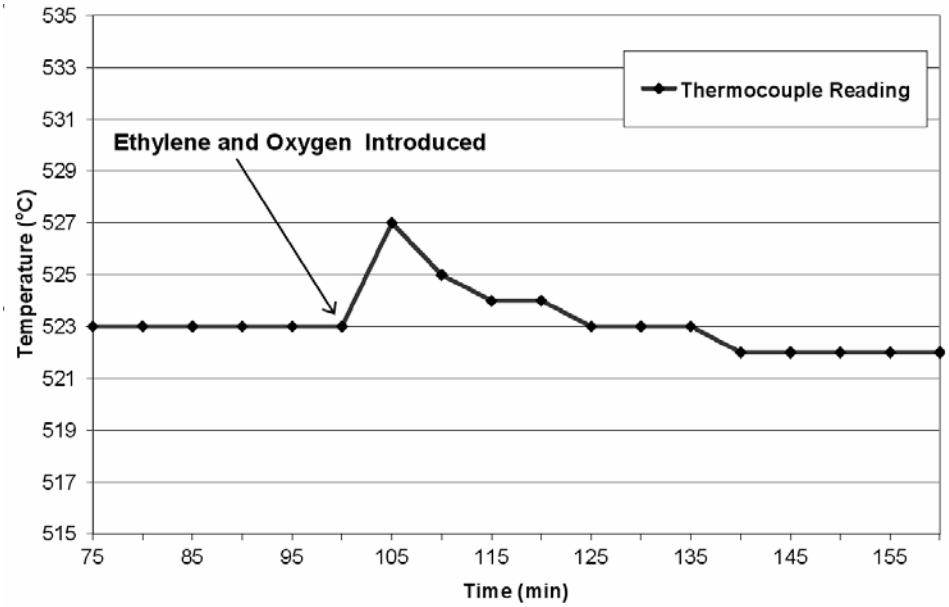

Figure 5 - Temperature profile during process conditions.

3.2.2 General Carbon Deposition Procedure

Carbon deposition was always accomplished via the catalytic decomposition of ethylene (C_2H_4). In addition to ethylene, oxygen and hydrogen were added to investigate the influence of secondary gases on resulting carbon deposition. In general, the reaction steps include:

1. Purge reaction chamber and heat furnace to desired temperature
2. Reduce samples with hydrogen
3. Second Purge
4. Reaction
5. Purge and allow furnace cool

For general deposition reactions, specifics of these steps are as follows: (1) The reactor is initially purged at 300sccm of ultra high purity nitrogen (99.9999%) while heating furnace to desired temperature. (2) At nominal temperature nitrogen (N_2) flow is stopped and replaced with a flow of 7% hydrogen in argon (99.99%). (3) The argon-hydrogen (Ar/H_2) flow is then replaced by 300sccm of N_2 to purge the reactor again. In the case of ethylene-hydrogen mixtures, this step may be omitted, since the next

(reaction) step will not necessitate the removal of argon-hydrogen from the reactor. (4) For the reaction, the N_2 flow is reduced to 300sccm and a chosen ratio of ethylene (chemically pure) to either oxygen (99.99%) or hydrogen (H_2) is introduced for a desired time. Typical flows for ethylene (C_2H_4) and oxygen (O_2) were 1:1 at 15sccm each. Whereas the O_2 used is undiluted with an inert gas, the H_2 is supplied from the same Ar/H_2 mixture used for the reduction step. Because of this, flows of H_2 were indirectly measured by the overall flow of the mixture. Hence, a mixture of 15sccm C_2H_4 with 50sccm Ar/H_2 yields an ethylene-hydrogen mixture of 15:3.5sccm or a 30:7 ratio by volume. This ratio was the standard mixture used for ethylene-hydrogen reactions. Gas flows for this standard reaction were controlled via mass flow controllers. Various parameters of the procedure (e.g. reduction length, flow rates, reaction times) were altered as needed for specific studies.

3.2.3 Fibrous Carbon Foam Reactor

To grow carbon foams a Lindberg 7" single zone tube furnace was used into which the entire reactor is placed. The reactor consists of two stainless steel tubes (0.250" O.D., 0.125" I.D.) which serve as the inlet and exhaust plumbing with the reaction chamber (mold) in the center. Gases were supplied using rotameters, and a check valve with 1.0psi crack pressure was placed in-parallel to relieve pressure once the mold becomes blocked with nanofibers. A general schematic of the apparatus is shown in Figure 6.

To create fibrous carbon foams of specific geometries a new reactor had to be designed. It had to meet several criteria in order to be a viable mold for carbon nanofibers. The first was a need to be stable under reaction conditions. This required it be inert to the gases used for fiber growth, and it had to be stable at reaction temperatures of 550-700°C. Secondly, it needed to be simple to produce and reliable for repeated use. Being that it had to be able to seal so as not to allow any gases to escape during the reaction and be created in-house meant the material had be easily manipulated and robust. To meet these requirements, stainless steel was chosen since it would perform in a satisfactory manner and was also cost effective.

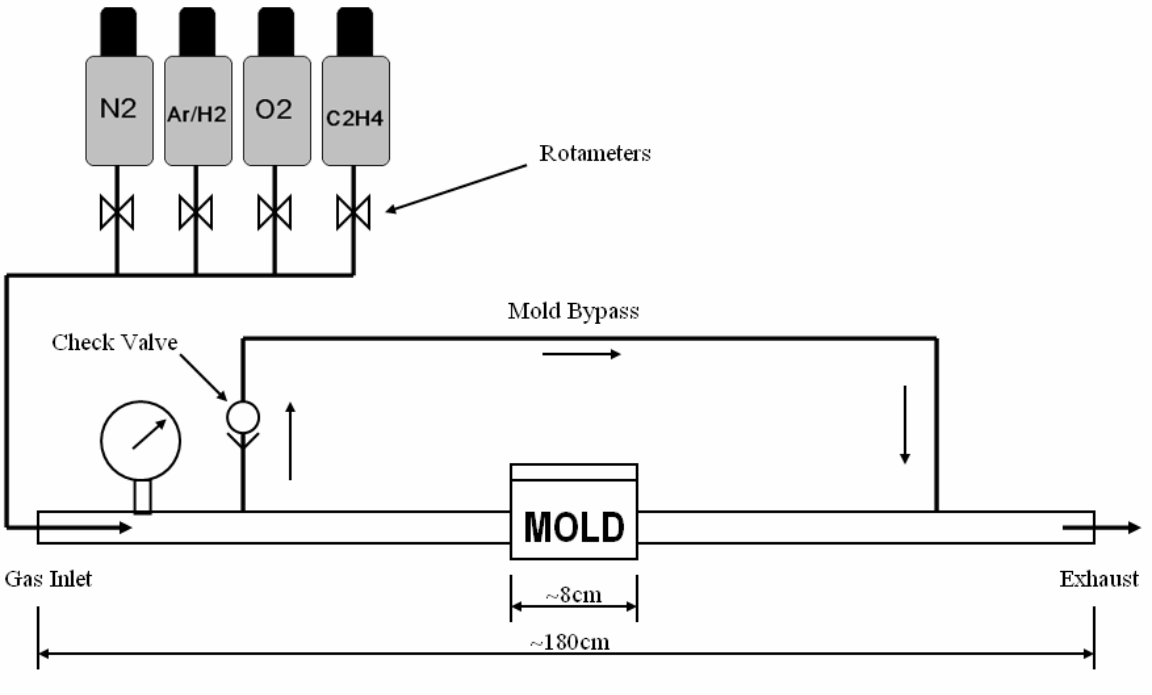

Figure 6 - Apparatus used in the growth of fibrous carbon foams

The mold itself is constructed of two major pieces. The first is the mold body, and the second is the lid. These two are connected by six stainless steel machine screws (8-32 UNC) fastened by stainless steel nuts. The mating surfaces of the body and lid were polished to ensure a tight seal under the conditions employed for carbon growth. Dimensioned drawings of the mold body are shown in Figure 7. In compliance with machining custom, the dimensions are provided in inches as to be conveniently reproduced if so desired. Thread specifications will have to be changed to a similar metric selection in keeping with uniformity of measuring system. The dimensions may be altered without significant impact to performance, and as will be detailed later, this is desirable for creating specific geometries. Because the mold is considerably smaller than the furnace diameter, a ceramic block was used to support the mold in the center of furnace cross-section, thereby reducing temperature irregularities.

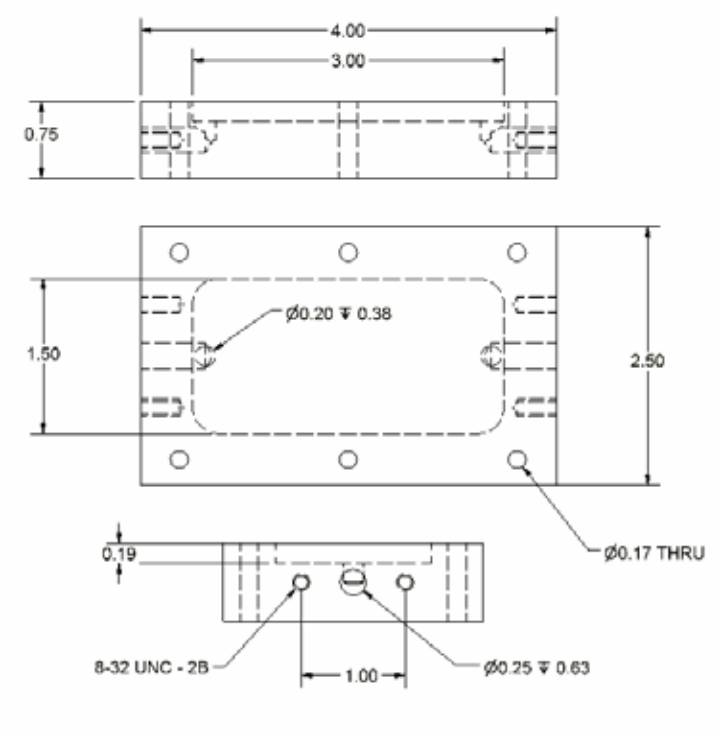

Figure 7 - Detail of mold body. All dimensions are in inches.

The stainless steel tubing used to plumb gases to the mold was secured to the mold body via stainless steel flanges. The tubing was welded to the flanges, and the flanges are fastened to the mold by two machine screws (8-32 UNC). As with the mold lid and body, the mating surfaces were polished to minimize leakage. A three-dimensional rendering of the complete assembly is shown in Figure 8.

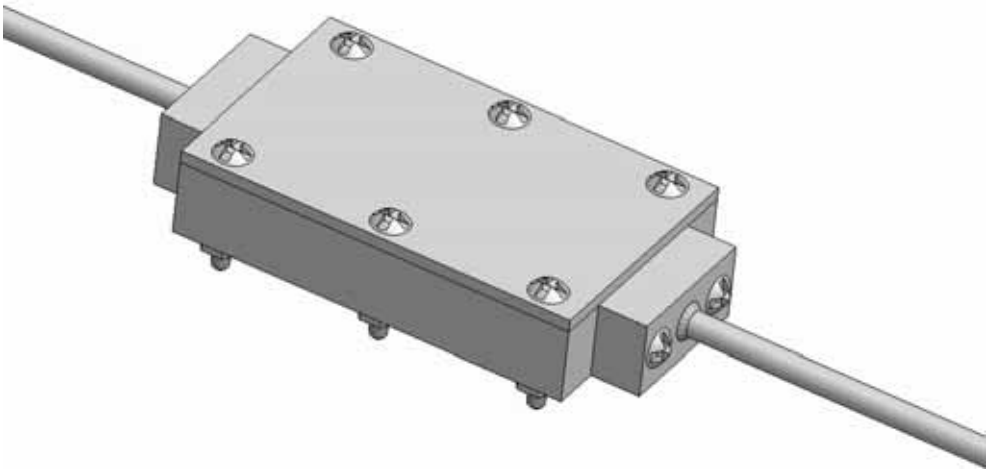

Figure 8 – Three-dimensional rendering of complete mold assembly.

As can be seen in Figure 8, the lid is dimensioned to match the mold body. For general reactions to create fibrous carbon foams, a lid 1/8" thick and flat on both sides was used to seal the reactor. This lid can be modified to investigate the ability to produce foams in more exotic geometries.

3.2.4 Fibrous Carbon Foam Procedure

Fibrous carbon foam reactions were carried out using the same procedure as general deposition reactions (Section 3.2.2). The major differences between the two are that the reaction was allowed to run until the mold was blocked, and the fibers were constrained during growth. The mold was cleaned using methanol, and a measured amount of palladium powder introduced. The amount and placement of the powder is important to determining the final properties of the foam. The temperature used was 550°C, but can be modified depending on the catalyst and gas mixture enlisted. The catalyst for this study was Pd sub-micron powder. Using less catalyst resulted in a longer reaction time, and denser foam as determined by measuring the volume of a section and measuring the mass. For example, 5mg of Pd sub-micron powder in ethylene-oxygen at 550°C would typically take 19hr. to completely block the mold. 20mg of Pd would do the same in 6hr or less under the same conditions. 3mg of Pd powder could take more than 2 days to block the mold, but the foam would be significantly stiffer. Composites were created by adding glass fibers with the initial palladium powder and processed as usual. To help distribute the powder for composites, the powder was suspended in methanol and added dropwise to the fibers in the mold, and the mold itself, including the lid. Adding the powder to the lid by this manner (allowing it to dry before assembling the mold) helped to center the fibers in the foam.

3.3 Characterization

To characterize the resulting carbon structures a variety of methods were employed. Scanning electron microscopy (SEM) was performed with a Hitachi S5200 Nano SEM to capture images of the as-deposited carbon and gain information on kinetics and morphology of growth. SEM and focused ion beam (FIB) studies were conducted

using a FEI Quanta 3D FEG microscope. High resolution transmission electron microscopy (HRTEM) was used to determine carbon structure with a JEOL 2010 at 200keV. Samples for TEM analysis were ultrasonically dispersed in ethyl alcohol and transferred dropwise to a 200 mesh holey carbon grid. X-ray diffraction (XRD) was used for crystallographic analysis using a Scintag PAD V X-ray diffractometer with Scintillation detector. Thermogravimetric Analysis was performed with a Netzsch STA 409 PC Luxx to examine growth kinetics and overall crystallinity was studied by means of temperature-programmed oxidation (TPO).

4 Results

During this work some universal observations were made. The first section highlights these generalities and then the two types of reactions are discussed: General Carbon Deposition and Fibrous Carbon Foam Reactions. General carbon deposition is the more extensive of the two main topics, and therefore is broken into sections based on catalysis by palladium in three different gaseous environments. Each of these sections is further divided based upon the catalyst form. These general reactions are then followed by the carbon foam results.

4.1 General Observations

Although the deposition behavior of carbon on the catalytic templates employed proved to be quite complex, there are some important, over-arching themes that can be extracted. These generalities include the effect of identity and template of the catalyst, the gaseous environment, the temperature of the reaction, the duration of the reaction, and residence time. The impact of each of these variables was never exclusive of the others, but the importance of each could be generally understood.

4.1.1 Importance of the Catalyst Form

Perhaps the most important consideration in determining the resulting carbon deposition is the catalyst form. The forms of palladium studied in this work include foil, sputtered film, and powder. The catalyst form will largely govern what conditions are suitable for fiber growth. Depending on the form the morphology of the carbon that deposits, the gaseous environment that works best, and the temperature range over which the catalyst is viable in depositing carbon will all vary. Generally, the larger templates (e.g. foil) had a tendency to form planar, encapsulating layers unlike smaller templates (e.g. nanopowder) which had a tendency to quickly form fibers.

4.1.2 Importance of the Gaseous Environment

For a single catalyst material and template form the carbon morphology could be differed with differing gaseous precursors. For example, using a mixture of ethylene and hydrogen instead of ethylene and oxygen raised the temperature where deposition was most efficient deposition and also increased crystallinity. However, the greatest growth rate achievable in ethylene-hydrogen was less than that found in ethylene-oxygen. The growth rate in ethylene alone was negligible at any temperature tested (up to 900°C). Growth rate and crystallinity are the two main factors impacted by the gaseous environment.

4.1.3 Importance of the Reaction Temperature and Duration

Typically, increased temperatures will result in an increase in reaction rate as predicted by the Arrhenius equation,[40] but the carbon deposition here always showed a maximum rate below its maximum viable temperature. The postulated reason for this is the production of radical gas species, and will be discussed in detail in Chapter 5. The outcome of this is that, even though carbon may deposit up to 800°C, the deposition rate will be greater at lower temperature (e.g. 600°C). It is not only the rate that is dependent on temperature, but the morphology as well. One catalyst template may grow nanofibers, film, or a mix of the two in a single gaseous environment by simply varying the temperature. Also, by holding all the aforementioned variables constant, including temperature, the morphology can change as a function of time. The most common result of longer duration reactions was to transition from planar carbon to fibrous carbon.

4.1.4 Importance of Residence Time

Residence time, or position, in the reactor is rarely studied with the growth of carbon nanostructures. Despite this, it was found to be quite important. As discussed in Section 3.2.1, the general purpose reactor used had a Gaussian temperature distribution from inlet to outlet. When running samples placed throughout the length of the reactor, the time which the gases have been in the reactor becomes important, and it was found

that, depending on position, and consequently residence time, carbon deposition would occur at a temperature at which it did not at a different position.

4.2 General Carbon Deposition

In comparison to iron or nickel, palladium is not typically reported as a viable catalyst for carbon nanofiber growth in literature. However, it proved to be a versatile catalyst in terms of growth rate, type, and temperature range. The variety of gaseous environments in which it catalyzes appreciable carbon deposition was found to be quite robust. The temperature range was typically between 450-700°C, but some forms worked at temperatures well above or below these. It worked well in ethylene-oxygen environments of various ratios, and in ethylene-hydrogen mixtures, but did not catalyze carbon deposition in ethylene alone, which may be partially responsible for its obscurity as a catalyst for carbon deposition. Since multiple forms were tested, it allowed for insight as to the effect palladium morphology has on deposition characteristics. Moreover, some forms were found functional in conditions in which others were not, so employing comprehensive experimental techniques allowed the unearthing of even discreet catalytic behaviors.

4.2.1 Palladium in Ethylene

The deposition of carbon was negligible on all templates of carbon at all temperatures tested here. In ethylene alone, the samples tended to only encapsulate with a thin layer of carbon even after 19hr. on stream. The initial encapsulation is believed to poison the catalyst, and thereby cease the catalyzation of any further deposition

4.2.1.1 Sputtered Palladium Film in Ethylene

In pure ethylene, carbon deposition was minute. The carbon deposition rate on was found to be approximately 10.5nm/hr., which is less than .001% of the rate found for mixtures of ethylene with oxygen or hydrogen. This highlights the dramatic influence a secondary gas is to the deposition rate as will be discussed in subsequent sections (See

Sections 4.2.2.3 and 4.2.2.4 for kinetics). Figure 9 shows the resulting deposition after running a sputtered film sample overnight (~19hr) in pure ethylene. Figure 9a shows carbon from the top and Figure 9b shows the cross section of the sample.

a) 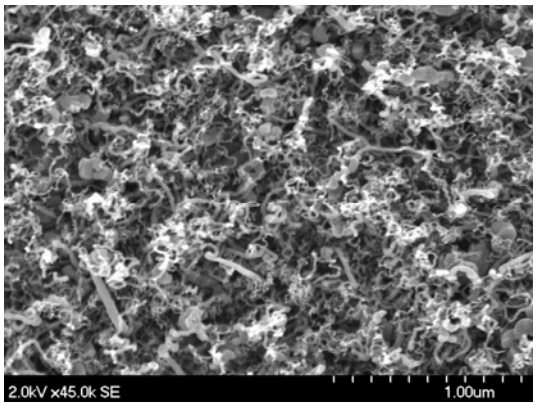

b) 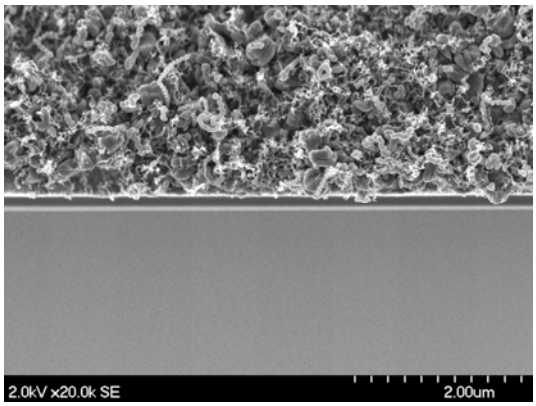

Figure 9 - Pd Sputtered Film after reacting overnight in ethylene at 550°C (a) top view at 45,000X magnification and (b) cross-sectional view at 20,000X magnification.

4.2.1.2 Palladium Foil in Ethylene

Palladium foil showed even slower growth and less surface coverage in pure ethylene than sputtered films. As Figure 10 shows, the carbon coverage of the foil surface is patchy and quite thin even after 19 hours. As will be detailed later, solid carbon films >1μm thick are achievable in under half an hour in the other conditions.

a) 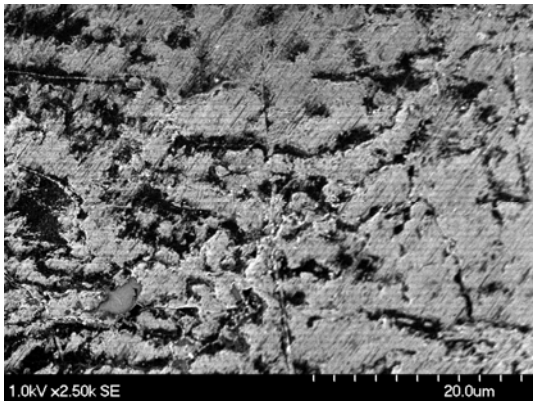

b) 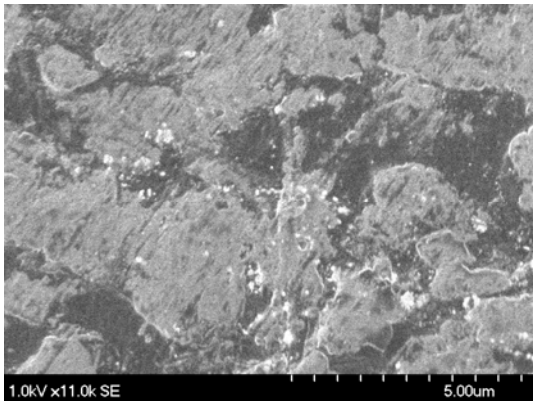

Figure 10 - Pd Foil after reacting for 19hr. in ethylene at 550°C at (a) 2,500X magnification and (b) 11,000X magnification.

4.2.1.3 Palladium Sub-Micron Powder in Ethylene

Palladium sub-micron powder, in manner similar to foil, was covered by a thin carbon layer after a 19hr reaction. The coverage on the sub-micron powder was more complete than on the foil as shown in Figure 11a. Figure 11b shows the backscatter image which reveals the particles below the carbon layer are close to the overall size indicating the carbon layer is quite thin.

a) 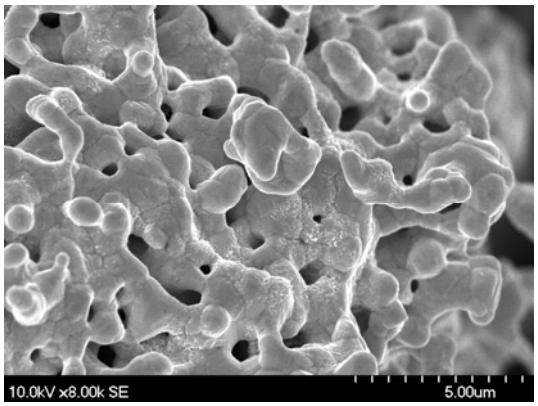

b) 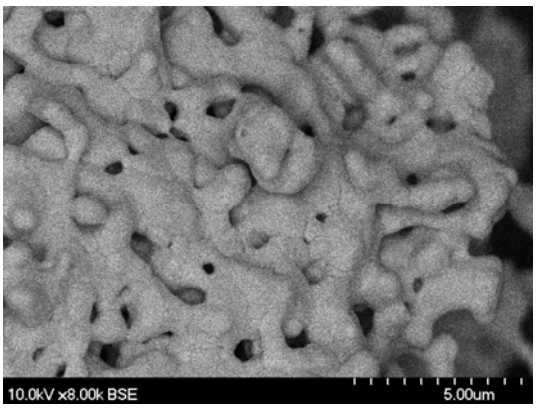

Figure 11 - Pd sub-micron powder after reacting for 19hr. in ethylene at 550°C at (a) 8,000X magnification and (b) backscatter image to highlight particles.

4.2.1.4 Palladium Nanopowder in Ethylene

As with the other forms, the carbon deposition on Pd nanopowder was planar and limited in extent. Nanopowder, like sub-micron powder, encountered encapsulation across the particle boundaries after 19 hours. Figure 12 shows this carbon encapsulation.

a) 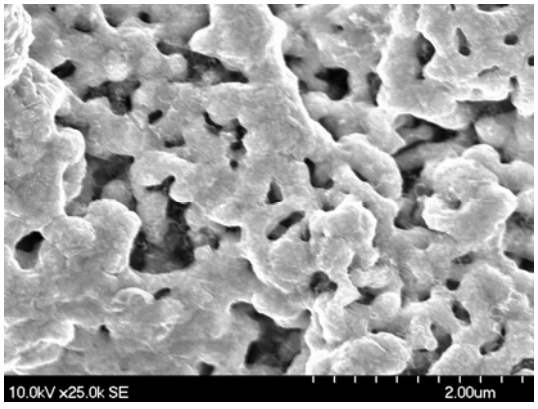

b) 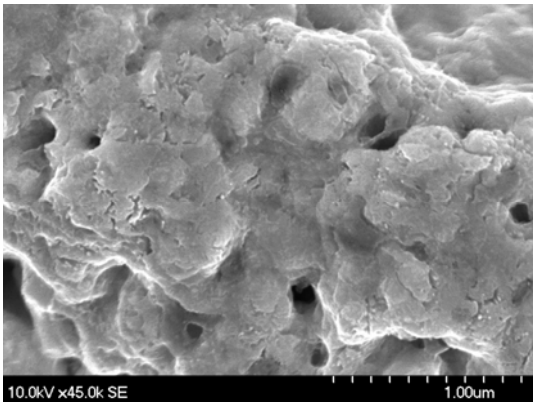

Figure 12 - Pd nanopowder after reacting for 19hr. in ethylene at 550°C at (a) 25,000X and (b) 45,000X magnification.

4.2.2 Palladium in Ethylene-Oxygen Mixtures

Unlike in pure ethylene, palladium was found to efficiently catalyze carbon deposition in mixtures of ethylene and oxygen. All forms were proficient at 550°C, a temperature at the lower end of most reported methods.[18,41] Sub-micron powder produced the most solid carbon out of all forms, and did so exclusively as carbon nanofibers. All palladium forms produced fibrous carbon with sufficient time or temperature, but palladium foil supported a brief period (~30min) of planar carbon deposition before transitioning to fiber growth.

4.2.2.1 Sputtered Palladium Film in Ethylene-Oxygen Mixtures

The sputtered film samples resulted in carbon deposition, in the form of fibers, over a broad range of reaction conditions. Fiber formation was seen in as little as 15sec with 15sccm of gas flow for C_2H_4 and O_2 (1:1) at 550°C. In addition to a quick onset, growth was remarkably fast, in some cases reaching nearly 3μm/min net height (i.e. measured thickness of the fiber film). This rate of growth was usually localized, with the center of the samples experiencing greater deposition than the edges. A typical growth rate is closer to 1μm/min for samples in the center positions of the furnace (i.e. 3 and 4). Actual fiber length was greater than net height, as the fibers twisted during growth.

Two features of the process of filament growth have a particularly strong impact on the final structure. First, the filaments pack together very tightly, especially when close to the film. Second, after a relatively short initial period (function of growth conditions) they do not grow directly up, but rather curve about as they grow. The net result is a tightly woven layer of intertwined filaments as illustrated in Figure 13. On a micron scale, the net result is a continuous, cohesive film. Indeed, observation at low magnification gives the impression of a solid film. Only high resolution observation reveals the fact that the film is composed entirely of fibers. Also shown in Figure 13a is the film layer delaminated from the substrate. The fiber mats are not chemically bound to the original substrate and are generally found to have delaminated as coherent structures after sufficient fiber growth. The Cr adhesion layer seems to be mostly inactive in the reaction, and provides support for the carbon nanofiber film formed by the Pd.

a) 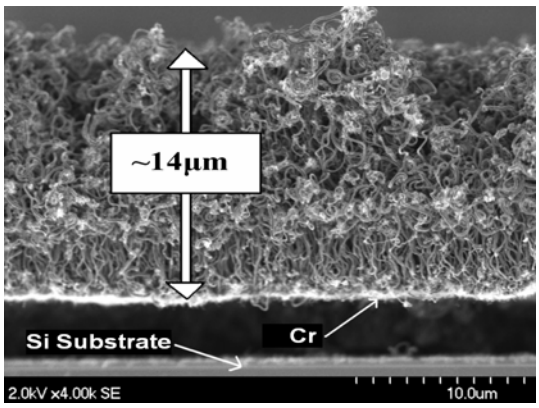

b) 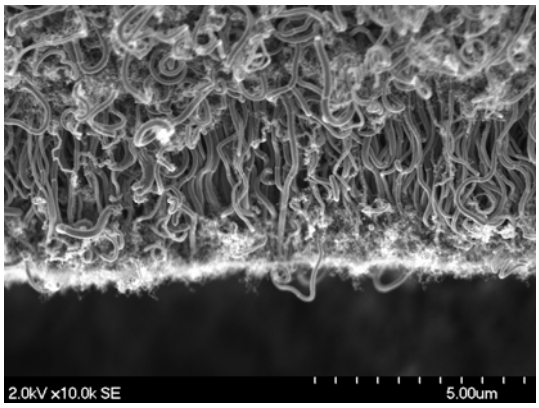

Figure 13 - Cross-sectional view of carbon nanofibers grown on a Pd sputtered film at 550°C nominal for 5min in position 4 with 15sccm of ethylene and oxygen each (1:1) shown at a) 4,000X and b) 10,000X. Refer to Figure 3 for positions, Figure 4 for actual temperatures.

Near the substrate surface the filaments grow vertically with a nearly uniform growth rate (Figure 14a). It appears that the diameter of each fiber matches that of the Pd particle catalyzing its growth. Backscatter electron imaging indicates the Pd particles are centered between two coaxial nanofibers and not at an end (Figure 14b). Shorter runs (<5min) tend to produce mats of aligned vertical fibers, but longer runs (e.g. 30 min), clearly produce mats with highly twisted, and randomly oriented fibers as shown in Figure 13a.

a) 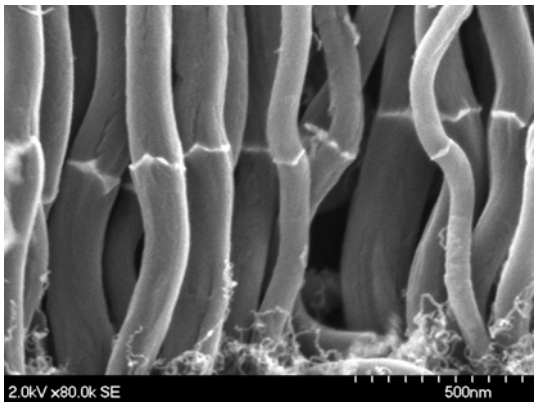

b) 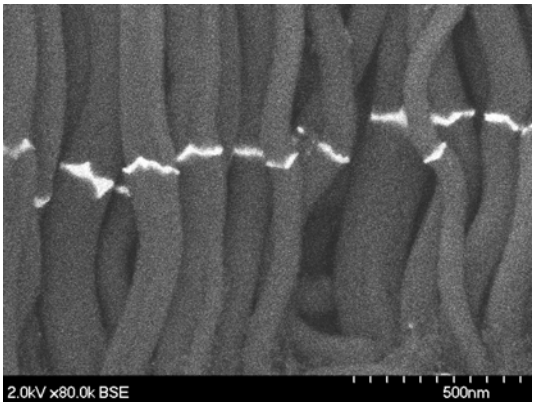

Figure 14 - View of carbon nanofibers at the substrate surface after 3min of growth at 550°C nominal in 15sccm each of ethylene and oxygen (1:1) in position 2 a) at 80,000X and b) backscatter image to highlight location of palladium particles. Refer to Figure 3 for positions, Figure 4 for actual temperatures.

Morphology of the fibers is impacted both by temperature and position within the reactor. At lower temperatures (e.g. 450°C), the carbon deposition tends not to consist of independent, easily identified fibers but rather an inchoate structure (Figure 15a). Even with considerably higher magnification than other images in Figure 15, it is harder to see clear fiber structure. At 550°C fiber structures form throughout the reactor, but the morphology is position dependent. In the center of the reactor well-defined, rapidly growing fibers form an interwoven film (Figure 15b), whereas at the end of the reactor the fiber density is clearly lower, and there is no coherent film structure (Figure 15c). Higher temperatures repeatedly produce thinner filaments (Figure 15d) which tend to have a tight, helical morphology.

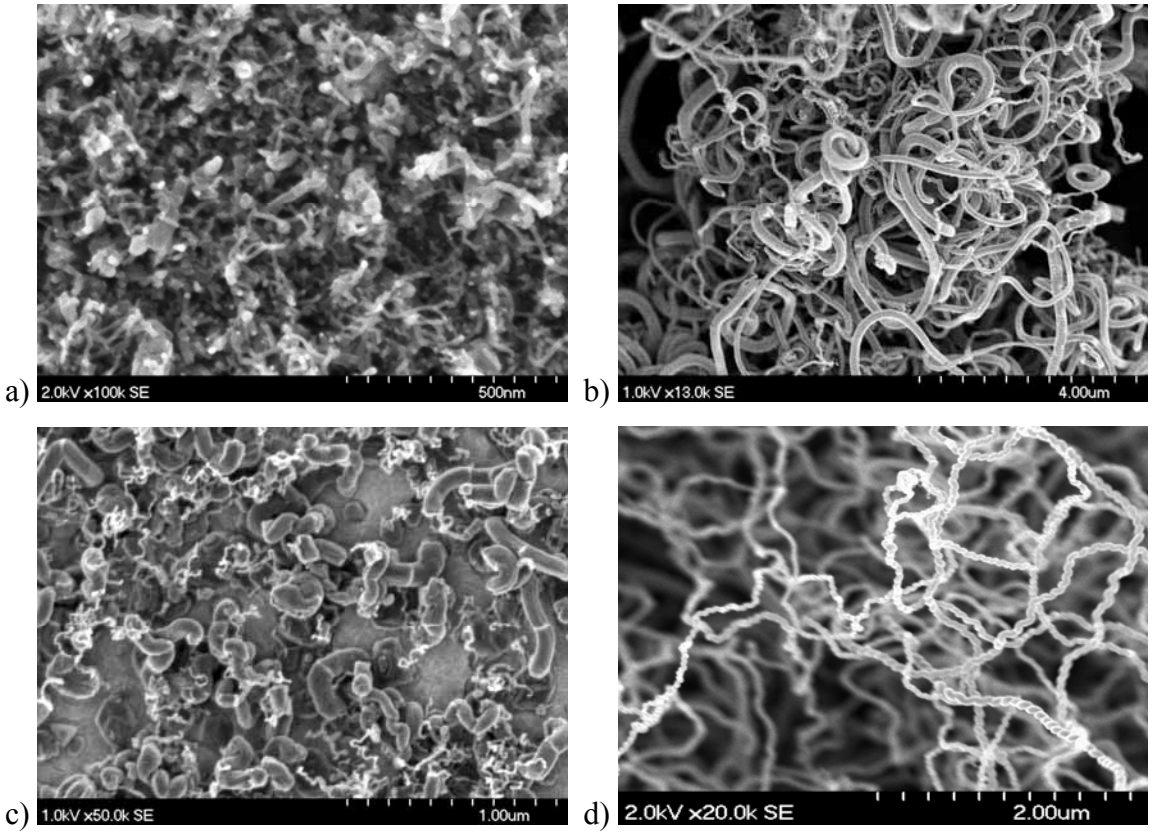

Figure 15 - SEM images of sputtered Pd film after 30min reaction time in C_2H_4 and O_2 (1:1) at 15sccm each. (a) reaction at 450°C nominal, pos. 3 (b) reaction at 550°C nominal, pos. 3 (c) reaction at 550°C nominal, pos. 6, and (d) reaction at 600°C nominal, pos. 3. Refer to Figure 3 for positions, Figure 4 for actual temperatures.

An effort to summarize the morphologies with respect to temperature and position is plotted in Figure 16. Some highlights are: (i) It is evident that growth at high nominal temperatures is favored toward the inlet. (ii) Growth at low temperatures is favored toward the outlet of the reactor. (iii) No growth is found above 700°C at any reactor position. This dependence on temperature and position suggests that growth is from radical species. It is notable that all three results (i.e. no growth, inchoate, and fibrous growth) can be obtained at a constant temperature (e.g. 375°C) or position (e.g. Position 3).

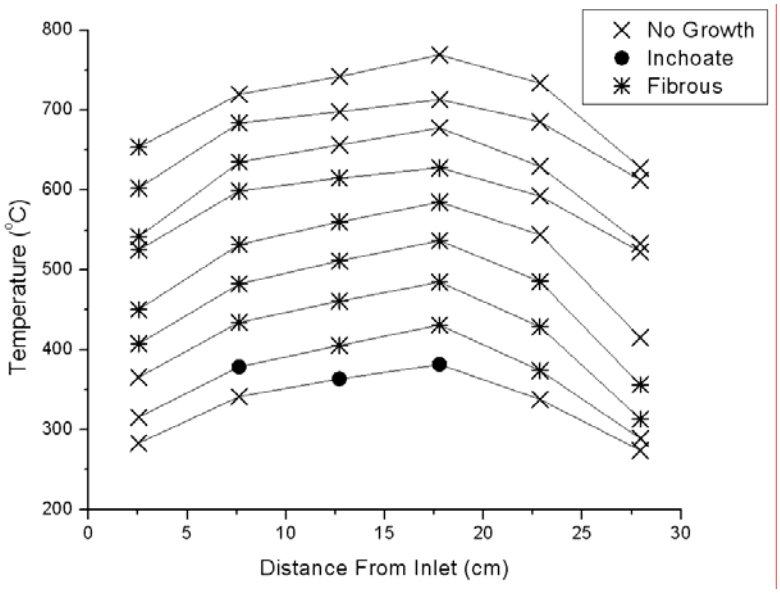

Figure 16 - Morphology plot for Pd sputtered film after 30min reaction time in ethylene-oxygen (1:1) at 15sccm each. Connecting lines indicate a single run at a nominal temperature. Distances correspond with positions 1-6 as shown in Figure 3. Temperatures based on Figure 4.

4.2.2.2 Palladium Foil in Ethylene-Oxygen Mixtures

The structures that form on foils are remarkably different than those produced on sputtered films even when processed side-by-side in the same reactor. Films of interwoven fibers formed on sputtered Pd films, whereas planar carbon films formed on the palladium foil.

Although planar films were dominant on foils treated for short times (<30 minutes), and low temperatures (<550°C nominal), some filamentous growth was observed after longer reactions or with temperatures above 550°C. Segments of the carbon film were severed by filaments breaking through after >30 minutes of treatment at 550°C. At temperatures below 550°C this incidence was less likely, and when occurring, less of the total surface was affected than at temperatures in excess of 550°C. At higher temperatures, the filament clusters were more pronounced both in the total surface area disturbed and the amount of fibrous carbon protruding above. This change in morphology is shown in Figure 17. Two samples from the same run are shown. Figure 17a was located at position 2 and Figure 17b at position 3. In position 2 there are few, if any filaments present with primary growth being flat, with the presence of fissures across the surface. The temperature varied by about 50°C between the two samples and emphasizes the importance on position in the furnace on resulting morphology.

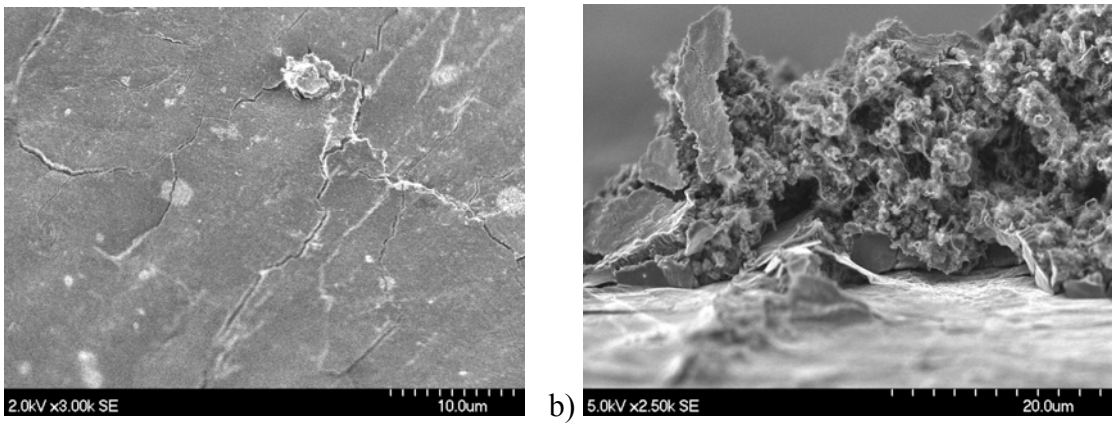

Figure 17 - Carbon deposition on Pd foil after 30min at 550°C nominal with 30sccm ethylene and 15sccm oxygen in (a) position 2 at 3,000X magnification and (b) position 3 at 2,500X magnification. Refer to Figure 3 for positions, Figure 4 for actual temperatures.

Cross sectional examination by SEM in tilt mode allowed for closer examination of the carbon structure as shown in Figure 18a,b. Once the carbon is broken it is possible to observe its structure more readily which illustrates a clear difference from fibrous growth.

a) 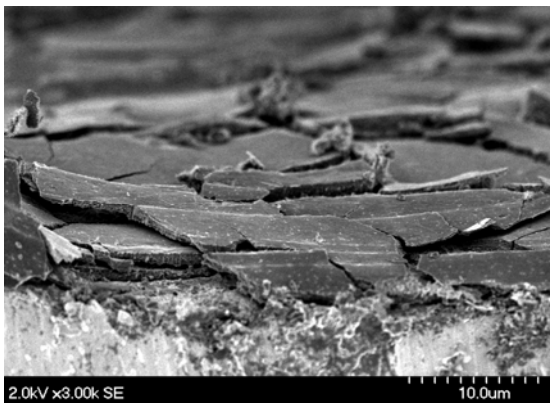

b) 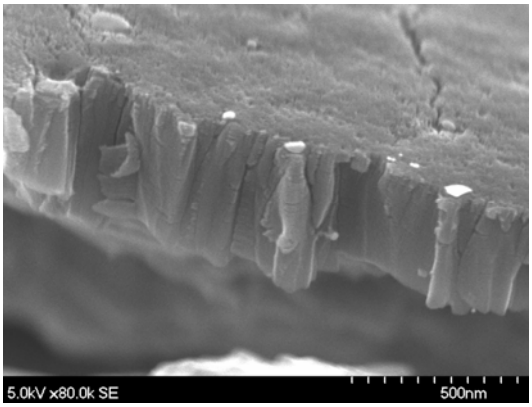

Figure 18 - Carbon deposition on Pd foil in 15sccm ethylene and oxygen (1:1) after 30min (a) at 550°C nominal in position 5 (3,000X magnification), and (b) a close-up of the film cross-section formed at 600°C in position 2 (80,000X magnification). Refer to Figure 3 for positions, Figure 4 for actual temperatures.

Similar to the sputtered films, the foil showed a variety of morphologies. As can be seen in Figure 19, the foil had a much narrower growth window than the sputtered films did. However, both forms showed a preference to growth toward the inlet portion of the reactor. Also, as was found for sputtered films, the foil samples showed a variety of results for single temperatures and single positions.

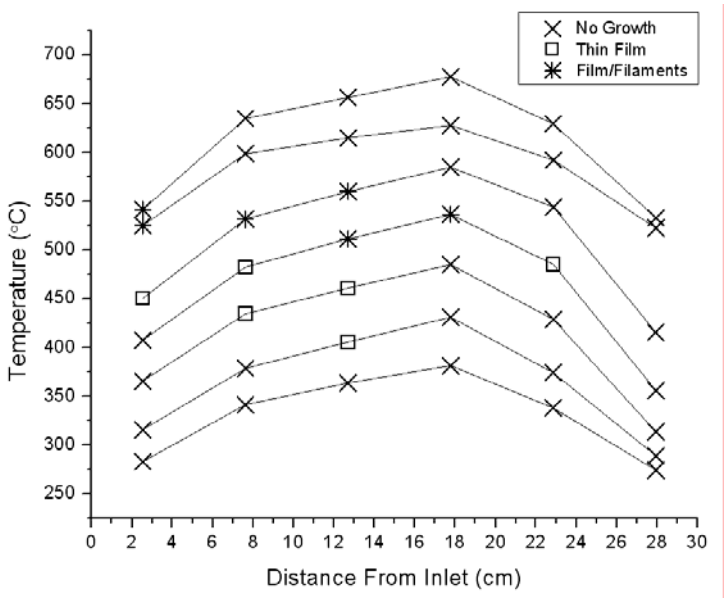

Figure 19 - Morphology plot for Pd foil after 30min reaction time in ethylene-oxygen (1:1) at 15sccm each. Connecting lines indicate a single run at a nominal temperature. Distances correspond with positions 1-6 as shown in Figure 3. Temperatures based on Figure 4.

4.2.2.3 Palladium Sub-Micron Powder in Ethylene-Oxygen Mixtures

Sub-micron powder was found to quickly catalyze carbon nanofiber growth over a large range of temperatures and gaseous mixtures. A 1:1 mixture of ethylene and oxygen at 550°C was found to be optimal for generating large quantities of carbon. Although sub-micron powder catalyzed great amounts of nanofibers, the growth was planar for a brief period before becoming fibrous (Figure 20a), although never totally planar as found with foil. After this planar period of growth, the morphology became entirely fibrous, and continued to grow for as long as the reaction was run, sometimes for several days.

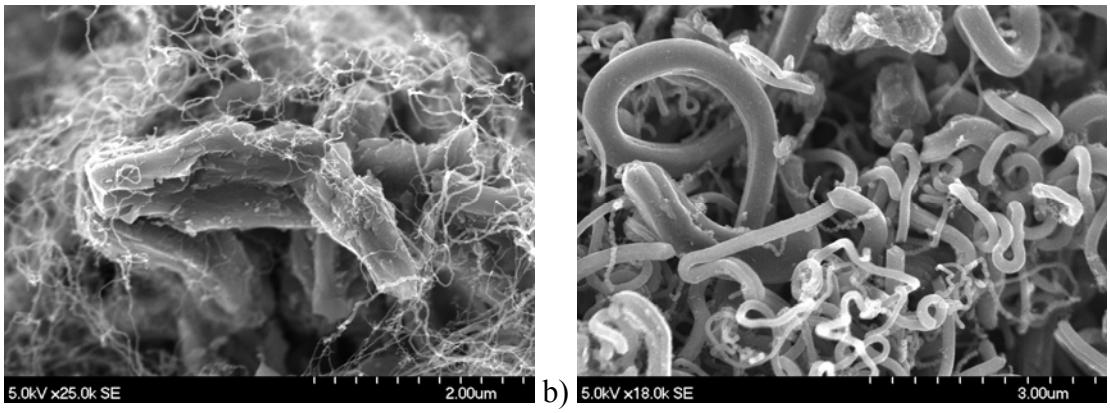

Figure 20 - Pd sub-micron powder in ethylene and oxygen (1:1) at 500°C after (a) 20min and (b) 1.5hr.

4.2.2.4 Palladium Nanopowder in Ethylene-Oxygen Mixtures

Palladium nanopowder was the final form tested here. The powder assumed morphologies analogous to the sputtered film samples. Fiber formation was seen at temperatures from 250-650°C but quite limited in extent at the extremes. Temperatures from 450-600°C were the most vigorous in carbon growth. Even with relatively little size distribution of the particles, fiber diameters varied significantly as shown in Figure 21.

a) 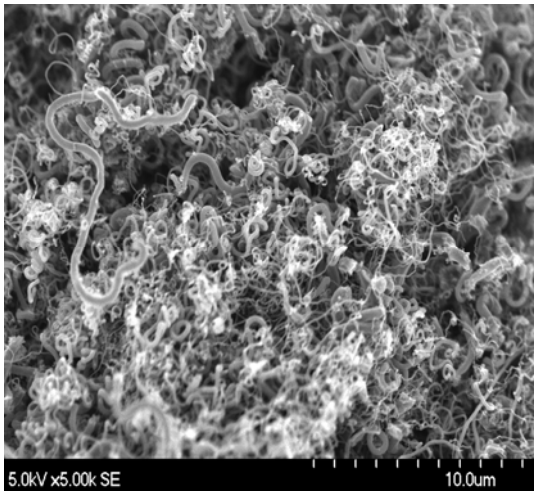

b) 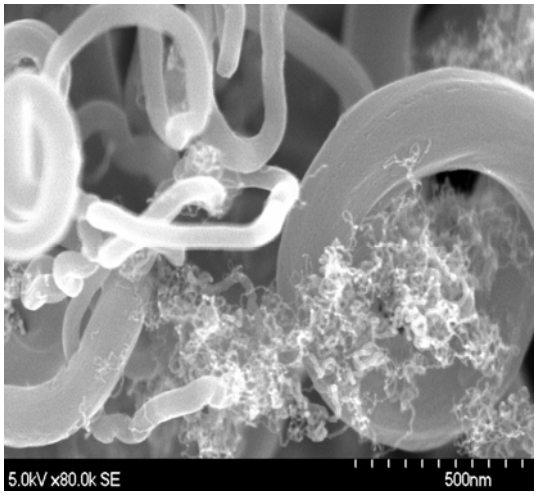

Figure 21 - Carbon nanofibers grown from Pd nanopowder at 550°C nominal in 50sccm C_2H_4 and O_2 (1:1) in pos. 4 at a) 5,000X and b) at 80,000X. Refer to Figure 3 for positions, Figure 4 for actual temperatures.

4.2.3 Palladium in Ethylene-Hydrogen Mixtures

Carbon deposition using ethylene-hydrogen mixtures proved to be significantly different than in ethylene-oxygen (combustion) mixtures. The maximum deposition rate occurred at a higher temperature for all forms in ethylene-hydrogen, and the morphology of the deposited carbon also changed. For some forms of palladium, a maximum temperature at which deposition occurred was not reached. The maximum temperature tested was 900°C, which is much higher than the maximum in ethylene-oxygen of 700°C.

For each run using ethylene-hydrogen, only one sample of each palladium form was used instead of six as with combustion mixtures. The center of the furnace was used in each run to closely correlate nominal temperature with actual temperature. Runs were conducted with samples side-by-side, and reactions were run for longer times because of a generally slower deposition rate. Because of this different approach morphologies are not listed in each section, but are summarized at the end (Section 4.2.3.5).

4.2.3.1 Sputtered Palladium Film in Ethylene-Hydrogen Mixtures

On sputtered Pd films nano-scale filaments (Figure 22) were the only structures generated, and only a firm lower temperature bound was found (~500°C). However, the absence of a firm upper temperature limit for growth is misleading, because as discussed later, growth slows dramatically above 700°C.

Given the general observation that the size of catalyzed fibers nearly matches the size of the particles that catalyze their growth as observed above and by others,[17,18,41] this suggests that the sputtered palladium films have short range order of a nanometer scale. Hence, the metal in the film tends to act in a fashion very similar to that observed for nanoparticles, catalyzing the growth of nanoscale filaments. Given that the palladium films were sputtered on and the fact that the films were not annealed, it is anticipated that the crystal structures in the films would indeed be on a nanometer scale.

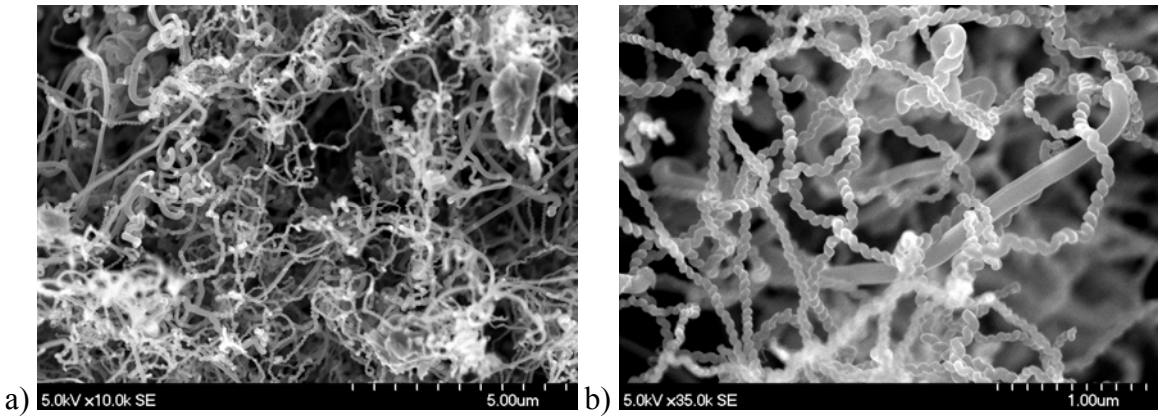

Figure 22 - Carbon nanofibers grown for 2hr. from Pd sputtered film at 550°C in ethylene-hydrogen (30:7) at (a) 10,000X and (b) 35,000X magnifications.

Several features of the fiber formation are worth noting. First, there appear to be two types of fibers. Many of the fibers are basically linear with intermittent kinks. However, more than half have a helical morphology when grown at 550°C. The origin of these different morphologies is not well understood, but has been attributed to a variety of mechanisms.[18,41] Considering the unique arrangement of the sputtered films (i.e. being in contact with a dissimilar metal), a support reaction with the underlying chromium adhesion layer may also introduce impurities leading to asymmetric carbon diffusion and

account for the increased presence of twisted fibers in comparison to fibers from other templates.[12] In a combustion environment, the presence of twisted fibers was also found to be dependent on gas ratio; increasing in occurrence at lower ratios of ethylene to oxygen.[42] When grown at 700°C the fibers formed tended to be more uniform in size and straighter than those deposited at 550°C.

4.2.3.2 Palladium Foil in Ethylene-Hydrogen Mixtures

As with all the other forms of palladium, carbon deposition on Pd foil in ethylene-hydrogen mixtures occurred over a limited temperature range. The range of appreciable growth was only between 600 and 700°C. At 550°C the deposited carbon film thickness was less than 5% of that observed at 700°C, and only partially covered the foil.

The primary form of growth was planar, but in all cases some rather sparse filament growth was observed as well. Figure 23a shows carbon film on Pd foil in ethylene-hydrogen after 1hr. of growth, and Figure 23b shows the carbon deposited after 2hr. Note the thickness dramatically increases with time indicating an increase in growth rate with time. It is also notable from Figure 1a that the films easily delaminate from the template.

a) 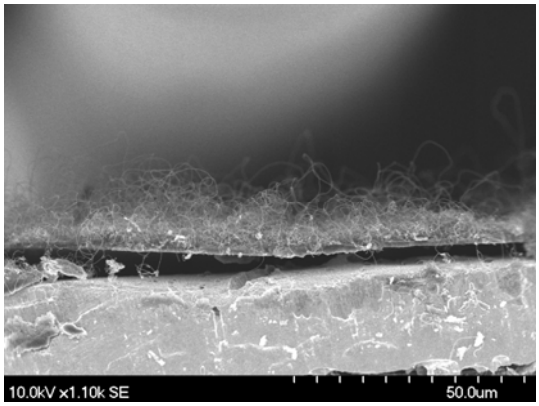

b) 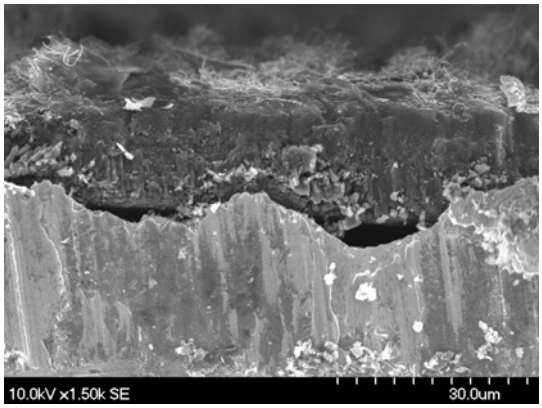

Figure 23 - Comparison of carbon growth on palladium foil in ethylene-hydrogen (30:7) at 700°C for (a) 1hr (1,100X) and (b) 2hr (1,500X).

4.2.3.3 Palladium Sub-Micron Powder in Ethylene-Hydrogen Mixtures

The lower limit temperatures at which substantial growth was observed on micron scale Pd particles was less than that observed for foils. Encapsulating structures were found to grow at temperatures as low as 500°C. However, the upper limit for growth, approx. 700°C, was the same as that observed for foil. Substantial fiber growth was only observed at 600°C and higher. Any fibers found at lower temperatures (Figure 24a) are clearly of a nano-scale, and probably grew because some particles in the 'sub-micron' Pd powder were in fact nanoscale. The fact that fibers were observed to grow on nanoparticles in this case is consistent with observations made with pure nanoparticle material (see subsequent section). From Figure 24b it can be seen the carbon encapsulating the Pd is thick enough to begin fracturing at what are presumably particle boundaries. At 700°C there was an increased fiber presence, but not nearly the quantity typical for sputtered film or nanopowder catalyzed carbon deposition (Figure 24c,d).

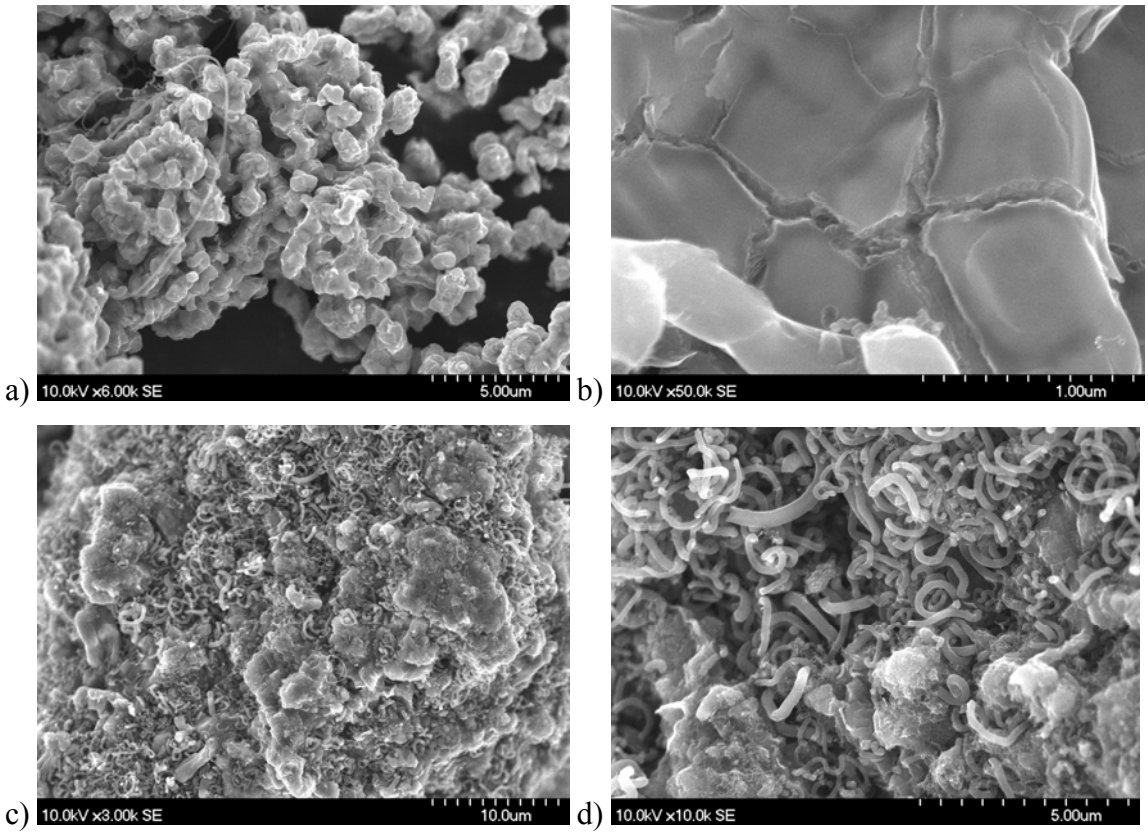

Figure 24 – Sub-micron Pd powder after 2hr in ethylene-hydrogen (30:7) at 550°C nominal (a) 6,000X and (b) 50,000X. and 700°C nominal at (c) 3,000X and (d) 10,000X.

4.2.3.4 Palladium Nanopowder in Ethylene-Hydrogen Mixtures

Similar to sputtered films, no upper temperature growth limit was found for Pd nanopowder in this study. The lower temperature limit (~500°C) is similar to that seen on the other forms of Pd. The morphology change with temperature on nanoparticles is essentially inverse to that found on sub-micron powders. That is, fibers grow rapidly at the low end of the temperature range, and an encapsulating structure forms at the high end. Under the same conditions that led to negligible growth on foils and encapsulation of micron scale particles, fibers grew rapidly on Pd nanopowder at 550°C and even faster at 700°C (Figure 25). At 700°C the fibers were more uniform in size and straighter than those grown at 550°C (cf. Figure 25a,b). A remarkable change in morphology is seen at higher temperatures (e.g. 900°C) where the growth transitions from completely fibrous to completely planar as particles are encapsulated by the carbon (Figure 25c,d).

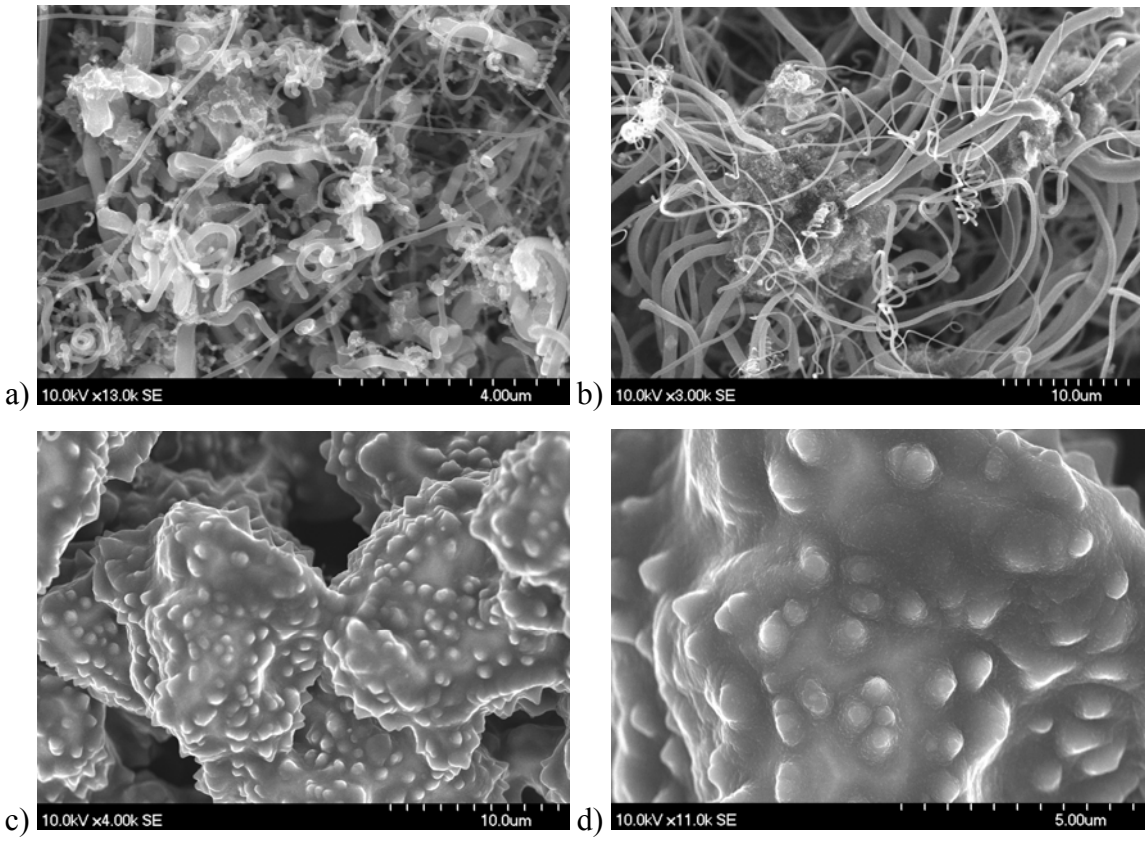

Figure 25 - Carbon deposition from Pd nanopowder in ethylene-hydrogen (30:7) after 2hrs at (a) 550°C (13,000X), (b) 700°C (3,000X), and 900°C magnified (c) 4,000X and (d) 11,000X.

Similar to a combustion environment, the key features of fiber morphology include: (i) In many of the fibers, the metal catalyst particle is in the center and not the end. (ii) The fibers often contain kinks and appear to change direction of growth with a few being helical. (iii) Arguably, the Pd particles are never fully encapsulated. (iv) Fiber growth is rarely seen at diameters greater than 300nm, however at 700°C there were a few exceptionally large fibers (>500nm), but these were scarce.

4.2.3.5 Morphology Summary of Carbon Deposited in Ethylene-Hydrogen Mixtures

Based on the above findings, the morphology of deposited carbon is plotted as both a function of temperature and Pd template in Figure 26. It is quite clear from this diagram that the pattern of morphology is quite complex, but there are some common features. First, fibers form on all templates, and second there is a lower temperature bound for growth on all templates. However, it is difficult to generalize further.

The importance of temperature is emphasized by the observation that for one template a variety of morphologies arise as a direct function of temperature. For example, planar structures form on all templates except for sputtered Pd films, but the temperatures at which they do are different for each. For mixed morphologies, the ratio of fibers and planar film varied with temperature as well. Specifically, foils produced a larger portion of fibrous carbon at 600°C than at 700°C.

Also notable is the effective temperature range of each catalyst. Whereas sputtered films and nanopowders were active for carbon deposition from 500 to 900°C, foil and sub-micron particles only maintained activity to 700°C. Foil, having the narrowest growth window of all the forms, did not begin appreciable deposition until 600°C. As discussed below in Section 3.6, the highest temperatures encountered reduced growth rates, and therefore it is expected that carbon deposition would cease soon after 900°C.

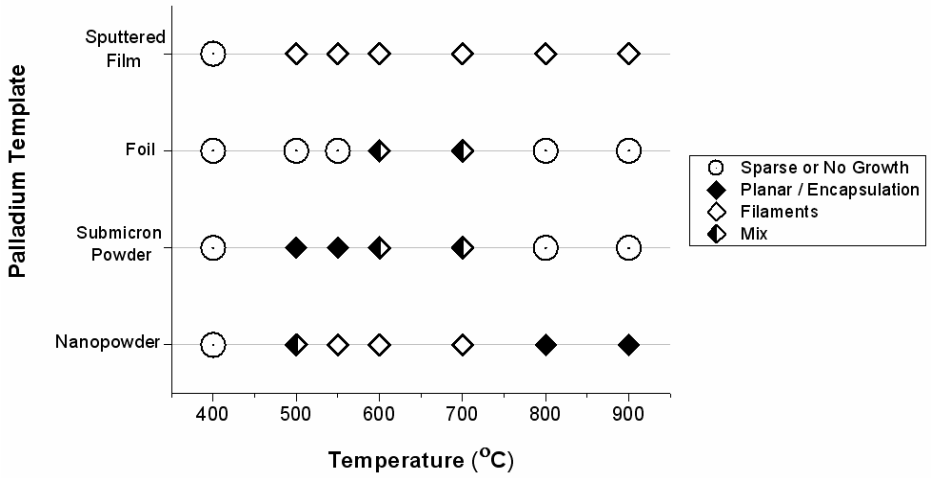

Figure 26 - Morphology plot of carbon deposited in ethylene-hydrogen (30:7) after 2hr. Morphologies labeled as "sparse or no growth" are less than 5% of those at 700°C.

4.2.4 Microstructural Study of Deposited Carbon

Crystallinity has an important effect on the properties of the resulting carbon deposition, so it was of interest to study what reaction parameters affected the overall atomic order. Under no conditions was highly graphitic carbon found to have deposited although factors such as gas mixture and temperature were found to be significant. The microstructure of the deposited carbon was investigated to ascertain its degree of crystalline perfection by means of x-ray diffraction (XRD), high resolution transmission electron microscopy (HRTEM), temperature programmed oxidation (TPO), and Raman spectroscopy. The factors adjusted were gas ratio, reaction temperature, and form of Pd. The Pd catalyzed carbon was then compared to carbon in the form of pyrolyzed sucrose, graphite flakes, graphite platelet nanofibers, multi-walled carbon nanotubes (MWCNTs) and single-walled carbon nanotubes (SWCNTs).

4.2.4.1 Microstructure of Carbon Deposited from Ethylene-Oxygen Mixtures

X-ray crystallographic analysis (XRD) was performed using a step size of 0.02° on 2θ and a dwell time of 1sec. for all data presented. Using XRD, it was found that all three forms of Pd produced various degrees of crystallinity, all of which have comparable crystallinity, namely very little. For all samples there was a broad peak centered around 25-26° on 2θ, typical for weakly defined, turbostratic graphite. Foil catalyzed deposition

produced the most crystalline carbon as determined by peak intensity and width, but by a nearly imperceptible margin. For longer runs, the foil lost some of its overall crystallinity. This may be attributable to a greater presence of filaments and a loss of graphitic film produced in the early stages of the reaction. In essence, the foil begins to assume a powdered form after long runs (>14hr.), because the Pd foil is effectively disintegrated and becomes mixed with the carbon filaments. Gas ratios of ethylene to oxygen from 3:1 to 1:2 had a negligible effect on crystallinity, with richer environments reducing crystallinity slightly. The temperature of reaction also showed little evidence of having a strong affect, but it did decrease crystallinity with decreased temperature. A 3:1 (C_2H_4:O_2) ratio at 550°C had a similar result to a (1:1) ratio at 350°C. The Pd template comparisons are shown in Figure 27.

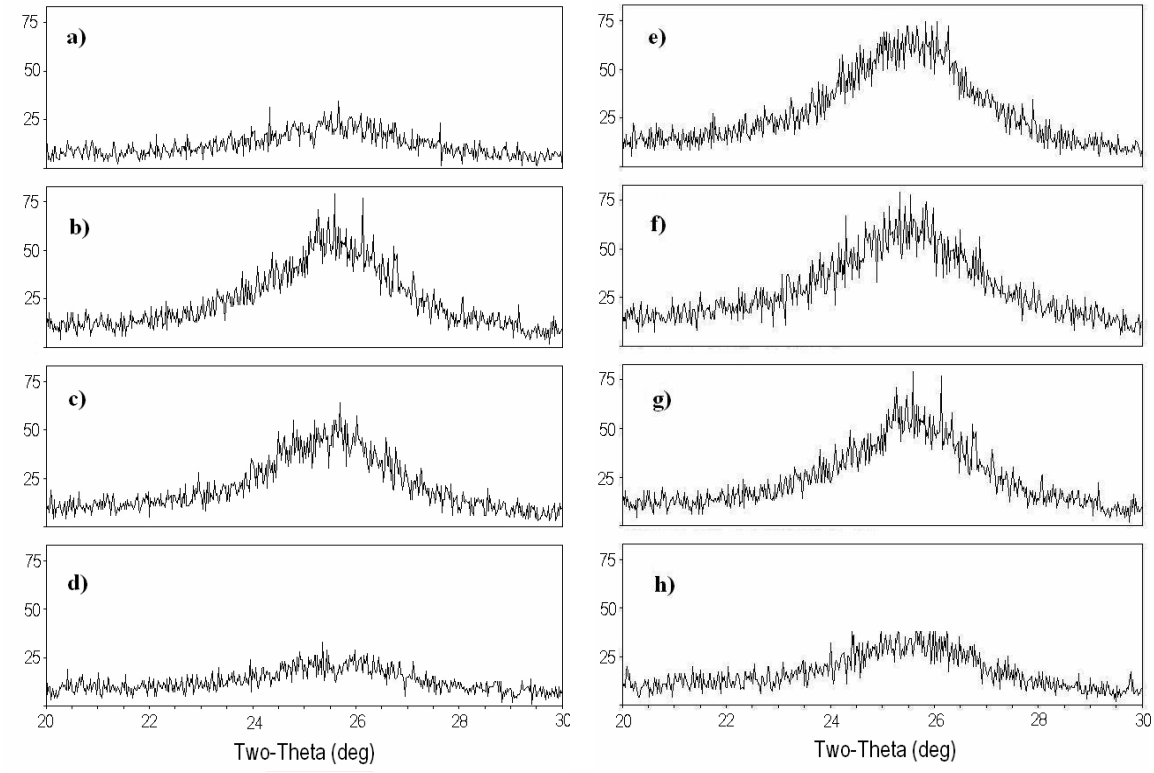

Figure 27 - X-ray data from 2θ = 20-30°, for CNFs from Pd sub-micron powder grown at 550°C nominal, in (a) 3:1, (b) 1:1, (c) 1:2 (C_2H_4:O_2), and (d) 350°C (1:1). Comparison of carbon catalyzed from (e) foil, (f) sputtered film, (g) sub-micron powder and (h) nanopowder all at 1:1 (C_2H_4:O_2), 550°C nominal.

Since all of the forms of palladium are very close to each other in crystallinity, it is difficult to gain any appreciable sense of their relation to highly oriented carbon structures (e.g. graphite), so the resulting crystallinity of the Pd catalyzed carbon was compared to graphite flakes, graphite platelet nanofibers, MWCNTs and SWCNTs. The limited crystallinity of the Pd catalyzed depositions becomes more apparent when plotted together with these other forms. As shown in Figure 28, the graphite platelet nanofibers are not as crystalline as graphite, but are significantly more crystalline than the Pd catalyzed carbon. Also, the Pd catalyzed depositions had peak maximums shifted down about 1° from the more graphitic forms. Even though carbon nanotubes are sheets of graphite (i.e. graphene) in tubular form, both types of carbon nanotubes appear limited in crystallinity because of the short range order intrinsic to graphite in the form of tubes.

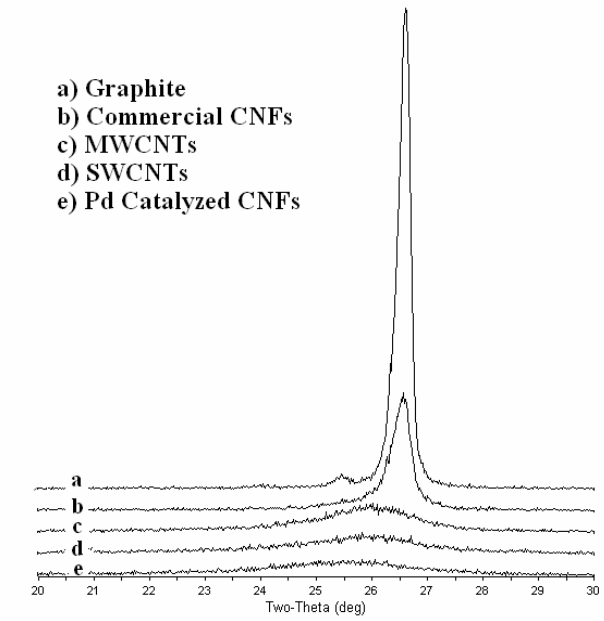

Figure 28 - X-ray comparison of a) graphite flakes b) graphite platelet nanofibers c) MWCNTs d) SWCNTs, and e) Pd foil catalyzed carbon

High resolution transmission electron microscopy (HRTEM) was the second method used to determine carbon structure. The lack of crystalline structure as found with XRD was confirmed by TEM analysis. Although there seems to be a hint of overall “herringbone” structure, there is no long-range order and no electron diffraction pattern created. The

typical atomic structure as seen in the TEM is shown in Figure 29. This structure was typical of all conditions and starting form of Pd.

a) 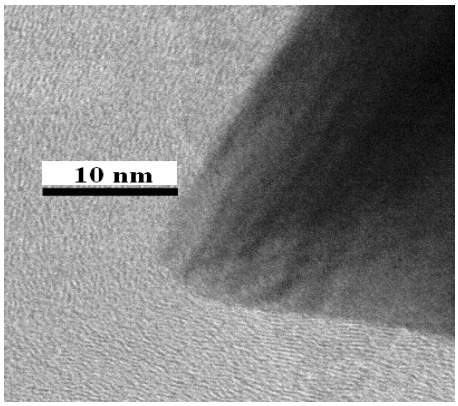

b) 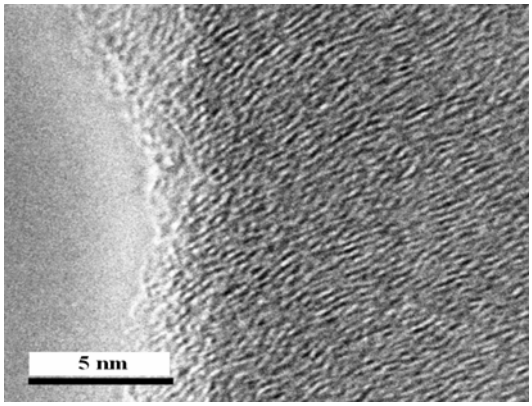

Figure 29 - Typical fiber structure showing little atomic order with a slight angle to the "planes" as a result of the catalytic particle shape a) particle in nanofiber (scale bar 10nm) b) Detail of atomic structure (scale bar 5nm)

Crystallinity was also examined using temperature-programmed oxidation of the samples in a simultaneous thermal analyzer (STA). A starting mass of 5mg of each carbon form was oxidized in 2sccm O_2 diluted with 40sccm of N_2. A temperature increase of 5K/min to a maximum of 900°C was used. To test for deleterious effects of Pd particles in the CNFs as noted by Wu et al. when activating carbon fibers doped with Pd,[38] the samples were oxidized with and without demineralization. To demineralize the fibers, they were immersed in Aqua Regia, sonicated, soaked for 7 days, sonicated again, rinsed with distilled water, and air-dried before oxidation. The particles proved difficult to remove, likely due to being almost entirely contained within the fiber. Even after extensive demineralization, there was still trace amounts of Pd present, although minor compared to unprocessed CNFs. Figure 30a,d are the same batch of fibers, one being demineralized (Figure 30d) and the other not (Figure 30a). The Pd clearly caused a lower activation temperature for oxidation, even below that of pyrolyzed sucrose. With the Pd removed, there was a much shallower slope indicating a variety of crystallinities, as was also seen with single wall carbon nanotubes, but to lesser degree. Any chemical alteration by the Aqua Regia would result in oxidation of the fibers which should not hinder additional oxidation during the temperature program. The oxidation behavior of the Pd catalyzed CNFs in Figure 30 are representative of carbon deposited by all forms of Pd studied.

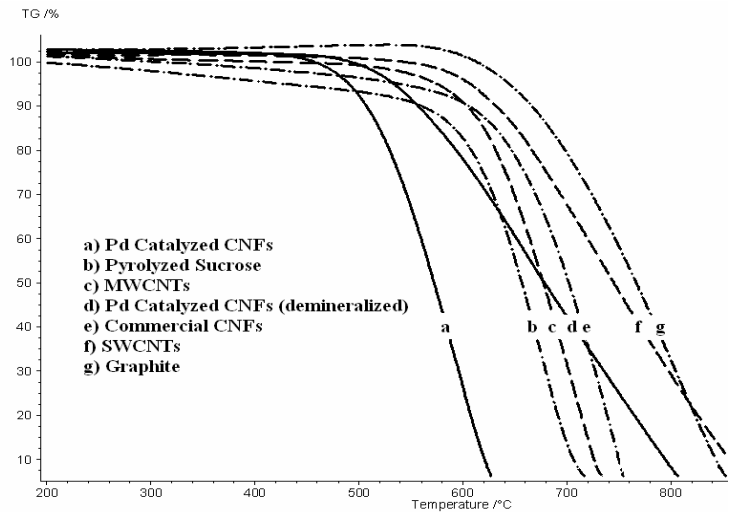

Figure 30 - Oxidation behavior of carbon as a) Pd catalyzed carbon nanofibers b) pyrolyzed sucrose c) multi-wall carbon nanotubes d) Pd catalyzed carbon nanofibers demineralized with aqua regia e) commercially purchased carbon nanofibers f) single wall carbon nanotubes, and g) commercially purchased graphite flakes

The commercially purchased carbon nanofibers (i.e. graphite platelet nanofibers) did not incur significant weight loss until much later than their Pd catalyzed counterpart. This indicates a higher overall crystallinity as was also found by x-ray diffraction. It is common for distinct sections of weight loss to occur at appreciably different temperatures when various crystallinities are present. A smooth line does not indicate this. Instead it suggests a uniform distribution of crystallinities ranging from totally amorphous to highly crystalline. Although minimal, the presence of residual palladium in the carbon cannot be excluded from consideration. Inherent complications such as this highlight the importance of using multiple methods when determining crystallinity.

The final method used in determining crystallinity was Raman spectroscopy. As before the Pd catalyzed CNFs were compared to graphite, pyrolyzed sucrose, graphite platelet nanofibers, SWCNTs, and MWCNTs. The comparison of these materials can be seen in Figure 31. Highly ordered and crystalline carbon materials (such as single-walled carbon nanotubes or highly oriented and crystalline graphites, as shown in Figure 31 a and c typically show very narrow characteristic "G" bands with frequencies between 1550 and 1600 cm^{-1}.[43] Additionally, defect and disorder-induced "D" bands occurring at frequencies between 1250 and 1400 cm^{-1}, are typically lacking or relatively weak in such

materials.[43-45] An increased presence of defects, disorder, and loss of crystallinity increase the relative D-band intensity with respect to the G-band, while simultaneously broadening observed line-widths,[43] as seen in Figure 31b, d, and f for multi-walled nanotubes and amorphous carbons. Once again it is evident that the carbon deposited by palladium is most similar to the pyrolyzed sucrose. The relative height of the D-peak and peak broadening signifies disorder to be high, but not quite as much so as the pyrolyzed sucrose. This correlates well with the other tests for crystallinity.

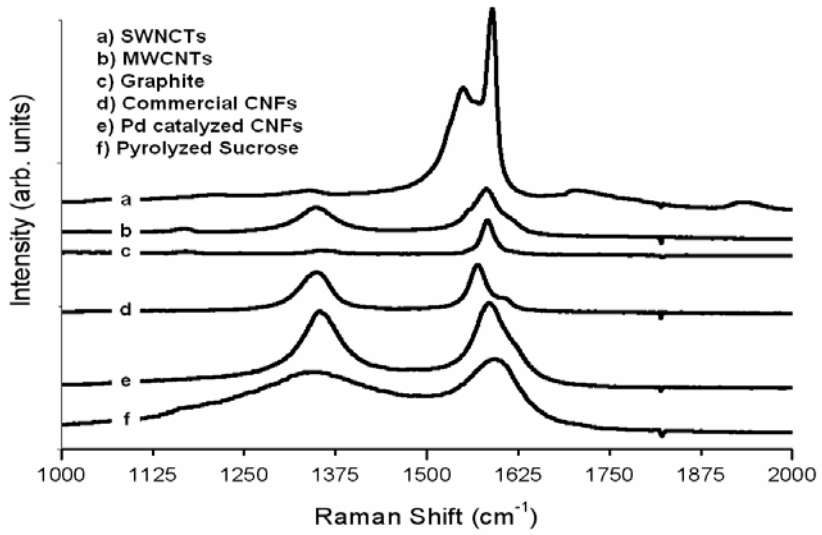

Figure 31 - Raman spectroscopy comparison of a) SWCNTs, b) MWCNTs, c) graphite, d) commercial CNFs, e) Pd catalyzed CNFs, and f) pyrolyzed sucrose

4.2.4.2 Microstructure of Carbon Deposited from Ethylene-Hydrogen Mixtures

Based on the microstructural study of carbon deposited in combustion mixtures, the analysis of carbon deposited in ethylene-hydrogen was restricted to the most effective methods of TEM and XRD analysis.

TEM and X-ray analysis revealed the carbon, from all templates, to be of limited crystallinity. This lack of crystallinity is similar to carbon deposited in ethylene-oxygen mixtures. The X-ray spectra from 15-35° on 2θ are shown in Figure 32a-d for Pd nano and micron powders at 550 and 700°C. The crystallinity improved slightly from 550 to

700°C in both cases. Pd nanopowder saw a somewhat higher and narrower peak at 700°C, and micron powder showed a low, broad peak instead of a nearly flat line. The lack of an appreciable peak for sub-micron powder at 550°C may be attributable to the lack of fibers and hence lack of viable carbon to produce a strong X-ray peak. This is supported based on the increased presence of fibers found when depositing carbon at 700°C. The fibers grown in ethylene-hydrogen showed improved crystallinity over those grown in an ethylene-oxygen environment, but the improvement was not drastic (Figure 32e,f).

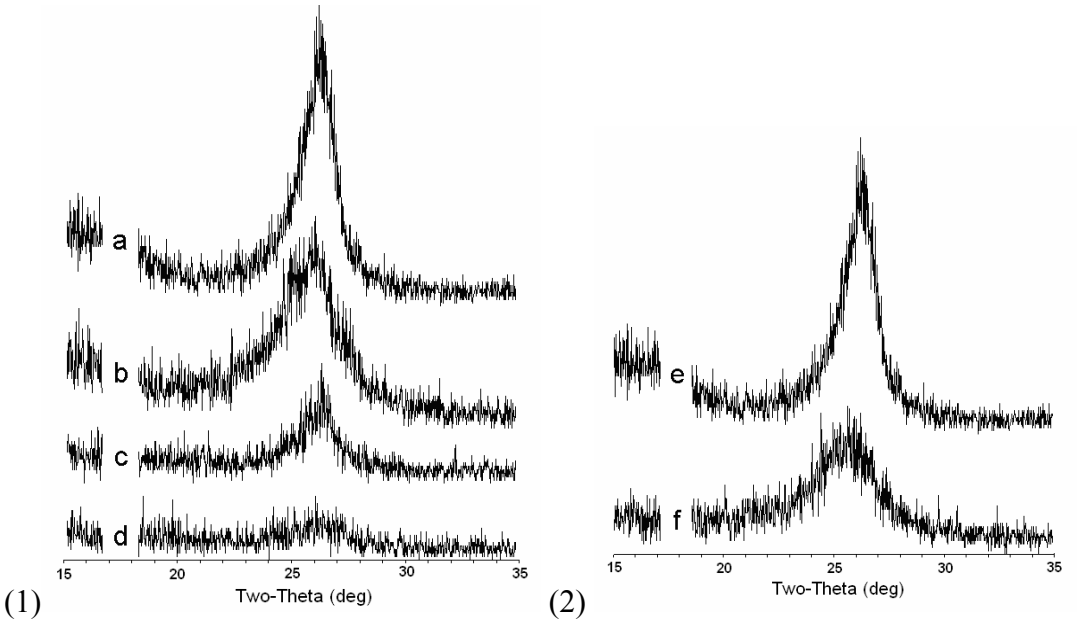

Figure 32 - XRD results for (1) Pd nanopowder at (a) 700°C and (b) 550°C, Pd micron powder at (c) 700°C and (d) 550°C, and (2) a comparison between Pd nanopowder grown in (e) ethylene-hydrogen and (f) ethylene-oxygen mixtures with other growth conditions being the same.

TEM analysis was consistent XRD results, confirming a lack of crystallinity in the as-deposited carbon at 550°C and an improvement at 700°C. Figure 33 shows a typical fiber distribution from Pd nanopowder (Figure 33a) and a detail of a twisted fiber (Figure 33b). Pd submicron powder resulted in particle encapsulation as shown in Figure 33c. A detail of the crystallinity, or lack thereof, is shown in Figure 33d. By raising the temperature to 700°C, the crystallinity was visibly better for both template forms (Figure 33e,f).

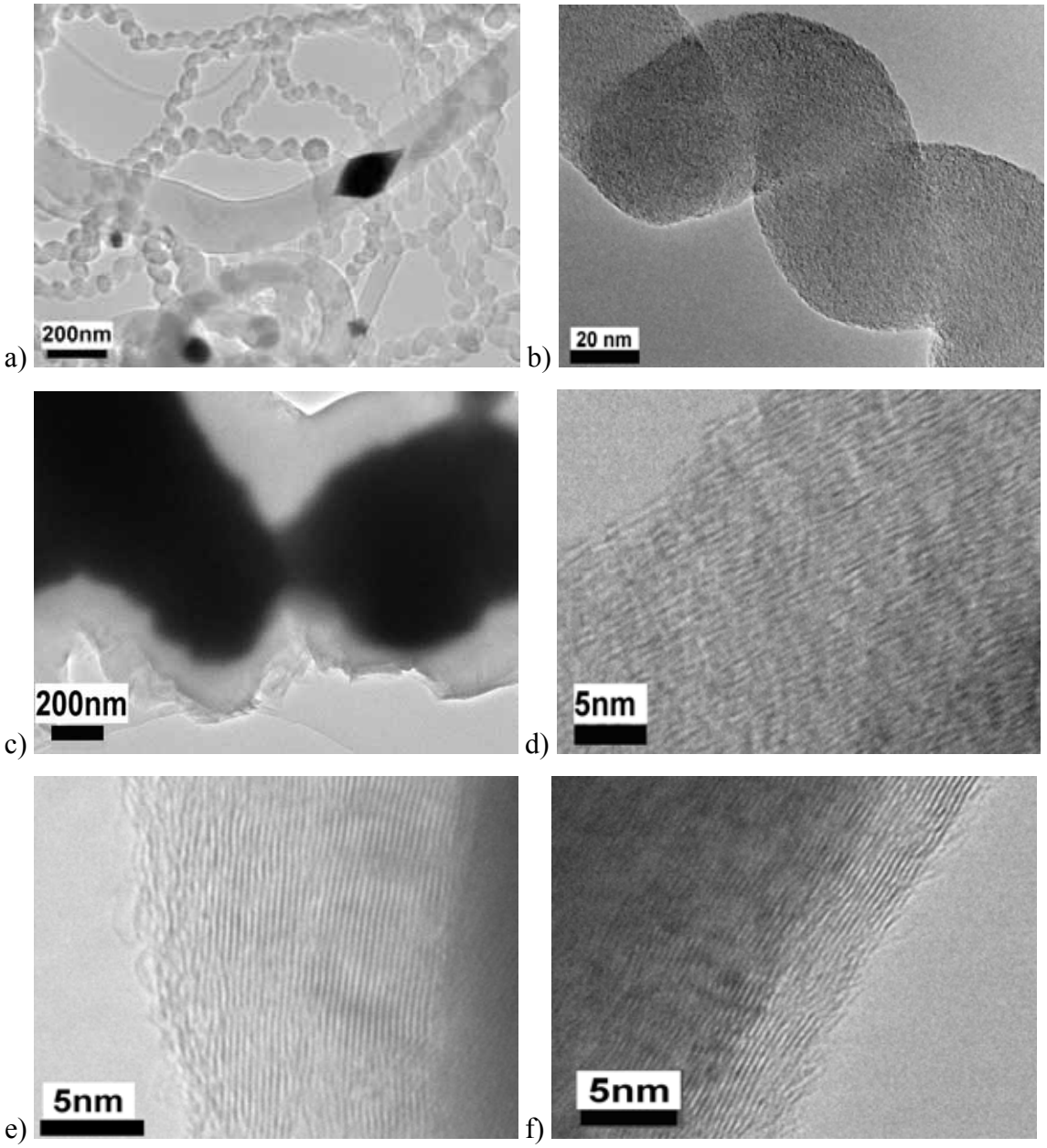

Figure 33 - Carbon deposition at 550°C for (a) Pd nanopowder with (b) detail of helical fiber and (c) Pd micron powder with (d) crystallinity detail. Carbon deposited at 700°C on Pd e) nanopowder and f) micron powder.

4.2.4.3 Kinetics of Carbon Deposited from Ethylene-Oxygen Mixtures

The kinetics of the deposition on various forms of palladium was of interest, especially the variation between planar and fibrous growth. To find the deposition rate as a function of morphology two forms were chosen due to the ease of which the carbon

growth could be measured, and the reliability of the morphology of that growth. These two forms were sputtered film (fibrous growth) and foil (planar growth). Profound differences in growth pattern both in terms of morphology and deposition rate were found. The film thicknesses, and consequently the growth rates, were established by cross sectional SEM analysis in the center of each sample. The sputtered film samples underwent a 5min. reaction at 550°C nominal in ethylene and oxygen (1:1) at 15sccm each. The average growth rate (of the fibrous "film") per position during this period is shown per position in Figure 34. No growth was observed in position 1. Growth, for sputtered film and foil, is approximated to be linear in time and the morphology constant while actively growing.

However, determining growth rates on foil samples is a more complex problem because the growth rates of both structures found changes with time. The planar structure grows rapidly, but steadily, at first, and then stops growing, whereas, filament growth only initiates after fifteen minutes or more and is thereafter remarkably rapid. However, it was possible to deconvolute the two rates based on the individual growth periods as found by analyzing samples at various intervals. These results are shown in Figure 34. In reviewing that data one caveat must be noted: The planar structures only grow to a maximum of about 1.5μm thickness, and then ceases to grow further. It was found that film deposition slows significantly near 1.5μm, and the growth then transitions to nanofibers which lift and break the planar structure. Moreover, the fiber growth rate, once initiated, is greater than an order of magnitude faster than the planar structure from the same Pd foils.

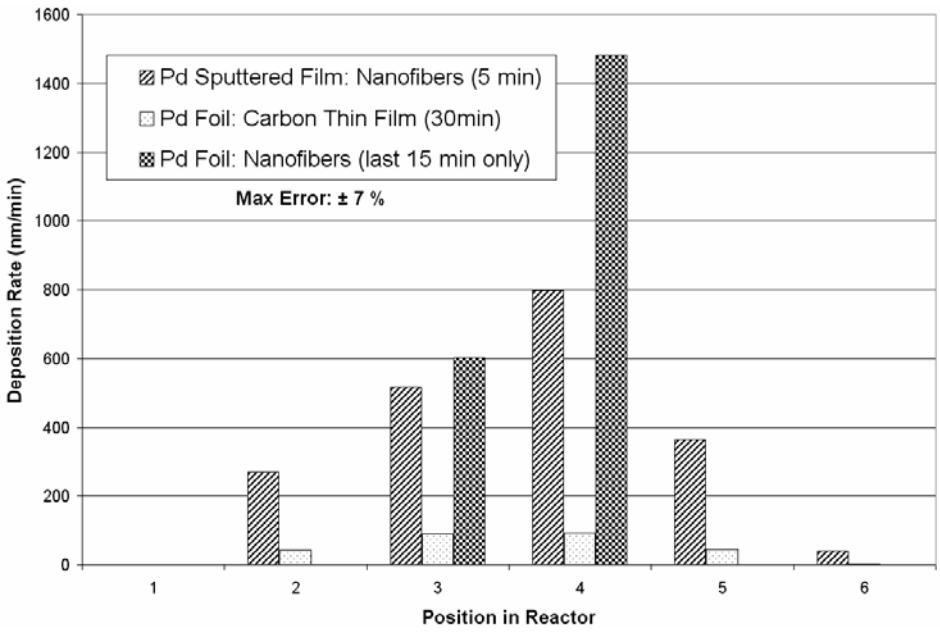

Figure 34 - Comparison of carbon deposition on sputtered Pd film and Pd foil at 550°C nominal in 15sccm C_2H_4 and O_2 (1:1). Refer to Figure 3 for positions, Figure 4 for actual temperatures.

4.2.4.4 Kinetics of Carbon Deposited from Ethylene-Hydrogen Mixtures

As with ethylene-oxygen mixtures, the rates of carbon deposition on sputtered palladium film and palladium foil were determined. The samples were run for 1hr. in ethylene-hydrogen (30:7) and are shown in Figure 35. Again, the thickness of the resulting carbon was measured by SEM cross-section analysis using the center of each sample. Thicknesses are typically greatest in the center, but the variation across the entire sample surface usually does not vary by more ±10% of the maximum. Samples on which significant growth occurs are usually more uniform than that of thinly covered samples. Samples were processed for 1hr., instead of 2hr. as done for the general study, in order to ensure the samples were actively growing throughout the reaction time.

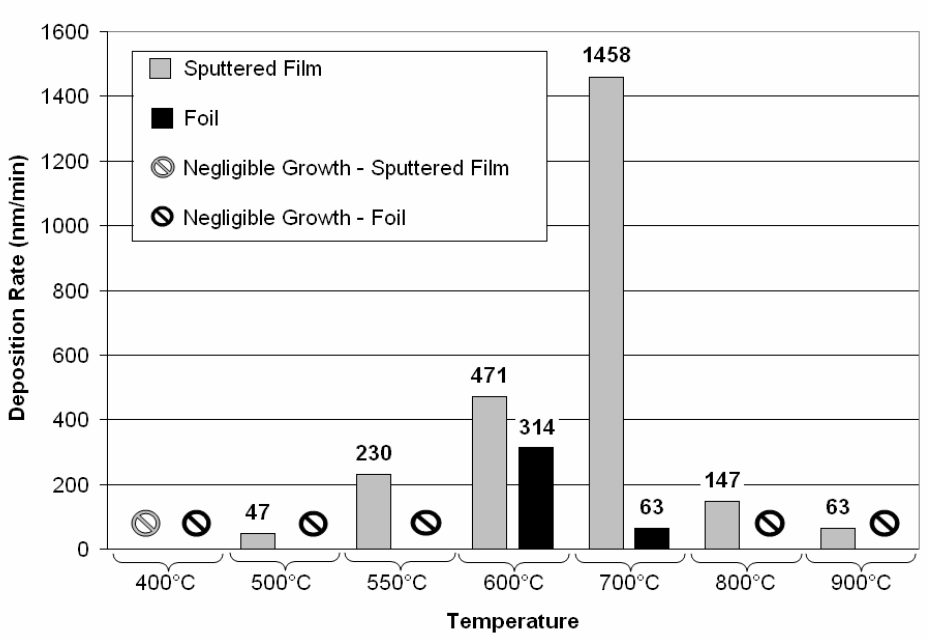

Figure 35 - Comparison of carbon deposition rate for sputtered palladium film and foil in ethylene-hydrogen (30:7). Samples were run for 1hr.

There is inherent difficulty in accurately determining the growth rate of fibrous films. Since the fibers are not exclusively vertical, the overall film height, or net height, is expected to be lower than actual fiber lengths. Also, some fibrous films do not experience a large rise in net height but create denser films. This was the case for sputtered film samples at 500 and 900°C. At 500°C the net height, and therefore the calculated growth rate, was less, but the film was denser and more uniform in height than at 900°C. Hence, it should be noted that the kinetics obtained serve mainly as a trend identifier and not as an absolute declaration of growth behavior.

For foils, since a mixture of fibers and film was present the growth rate includes both. Fiber growth was not as extensive as that found in ethylene-oxygen mixtures, but it did contribute to overall thickness, and the two were not as definitively separated as found in the combustion reactions, so they are not delineated in the growth rate shown in Figure 35. The mixed growth mode makes it difficult to accurately determine rate. Therefore, the carbon film growth rates are likely to be lower than the combined rate since fiber growth is consistently faster.

As with ethylene-oxygen mixtures, the growth rates are assumed to be constant throughout the 1hr. growth period. However, the rate does vary with time, and it does so differently for foils and sputtered films. With respect to time, the growth rate for carbon on sputtered film was found to decrease with time, but the rate increased for foil samples. This may indicate a discrepancy in growth patterns where sputtered films begin growth quickly and slow down with time, and contrary for foils, growth rate may either increase with time or there may be an initial induction period before growth begins. Due to the complexity of the mechanisms, only the average growth rates are reported here. Further studies will be required to elucidate details of the kinetics.

4.3 Fibrous Carbon Foams

Fibrous carbon foam composed entirely of fibers is a novel material, and can be accomplished relatively quickly and simply using a modified general deposition procedure. As found in the general deposition reactions, Pd sub-micron powder in a 1:1 mixture of ethylene and oxygen at 550°C proved to be the most prolific at carbon generation. This palladium form was then utilized using the fibrous carbon foam process (Section 3.2.4) to produce a coherent billet of carbon foam. From this billet the bottom left corner was removed using scissors for SEM analysis. The results of the SEM analysis showed the foam to be entirely fibrous. A progressively increasing magnification of the foam is shown in Figure 36a-f, and reveals the truly fibrous nature of this foam.

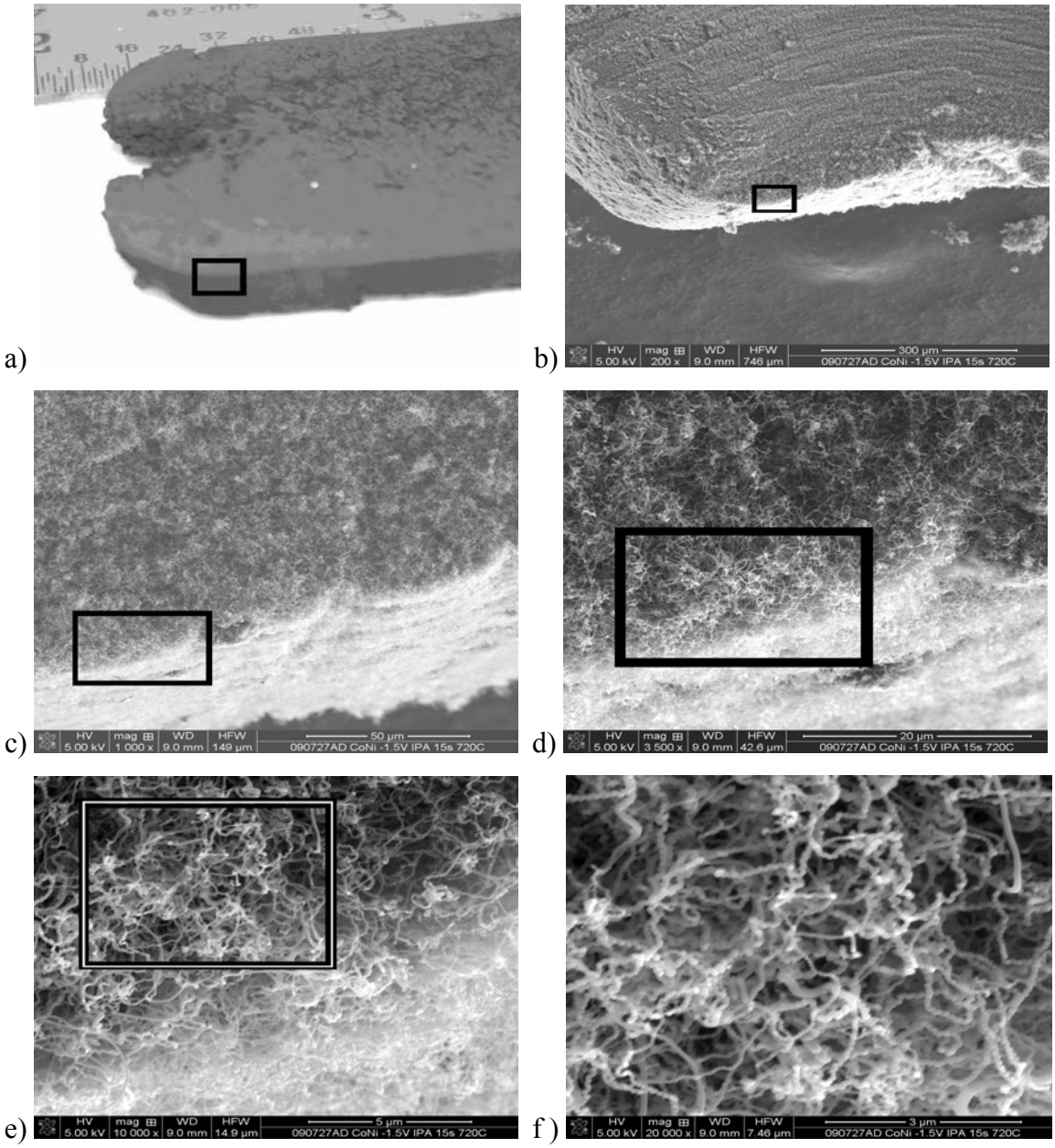

Figure 36 – Fibrous Carbon Foam at increasing magnification, boxes indicate section in next image (a) 1X (b) 200X (c) 1,000X (d) 3,500X (e) 10,000X (f) 20,000X

Using a focused ion beam, sections of foam were milled to allow for evaluation of the foam's interior. An example of the resulting section is shown in Figure 37a-d. As before, the fibrous nature is apparent, and the fiber density is high, although the bulk density is not.

a) 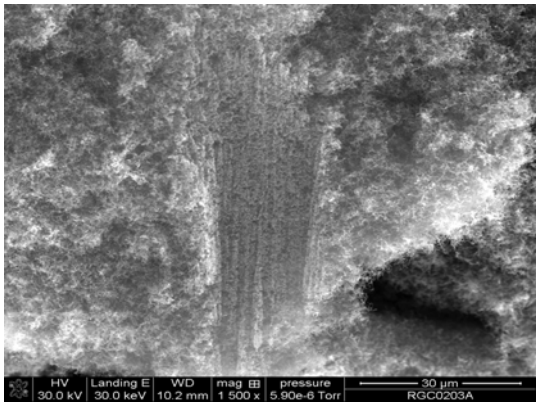

b) 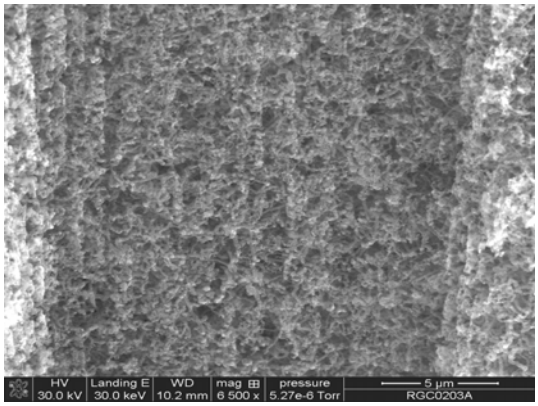

d) 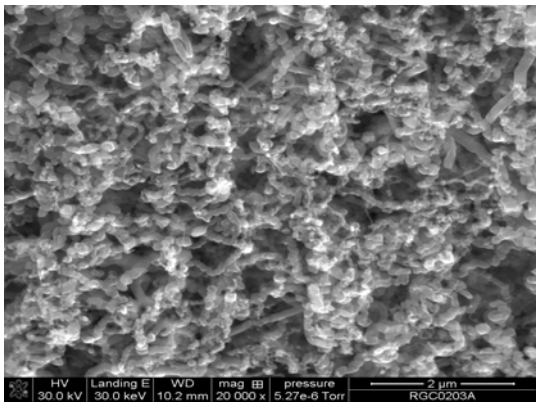

e) 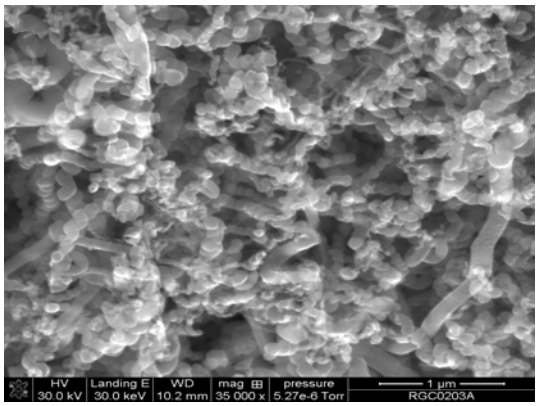

Figure 37 - Cross section of carbon foam at (a) 1,500X (b) 6,500X (c) 20,000X (d) 35,000X

Using the aforementioned process a billet of carbon was formed (Figure 38a). Aside from being lightweight, the foam was found to be flexible and resilient. It was repeatedly bent past 90° (Figure 38b) and would retain curvature after a bit of elastic recovery. In its plastically deformed state it could support small loads without returning to its original, flat dimensions (Figure 38c,d). However, it could be flattened again without cracking or disintegrating.

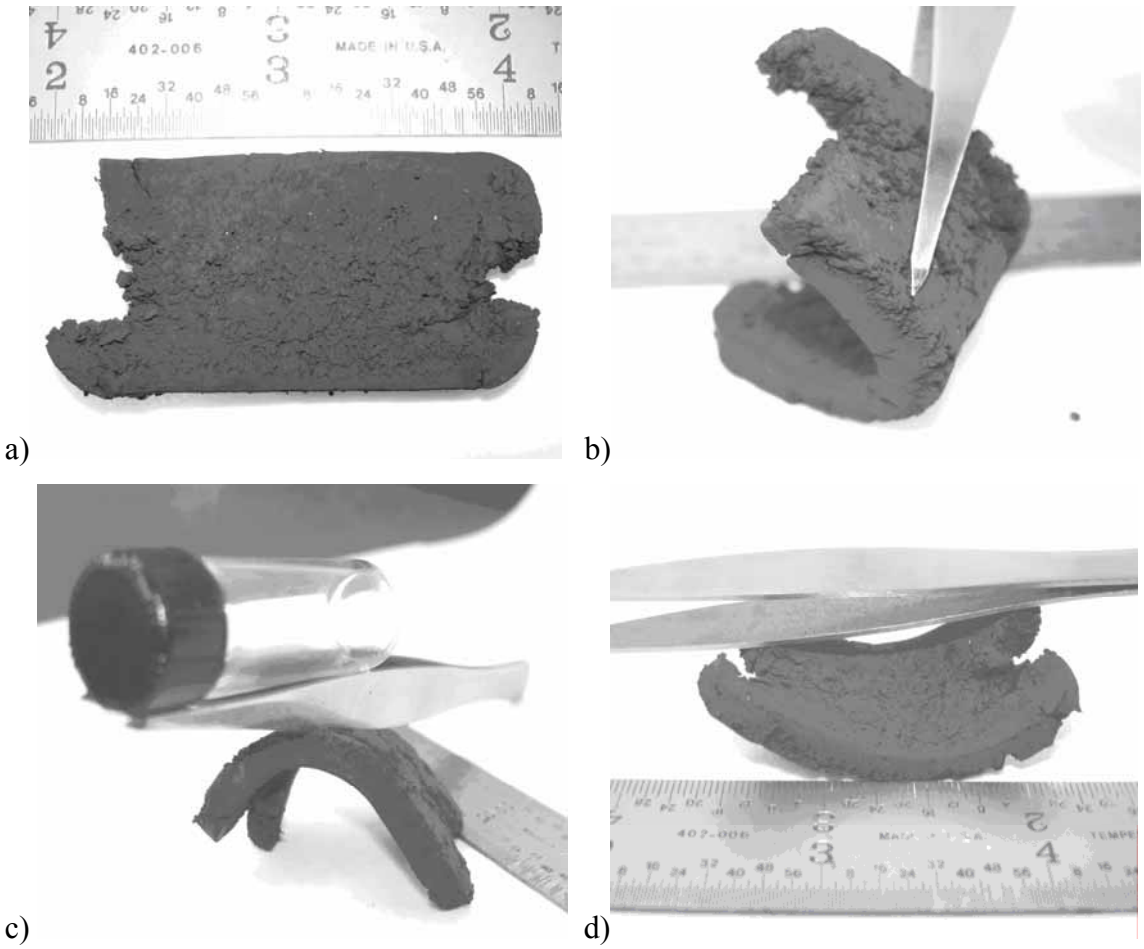

Figure 38 - Carbon Foam (a) as removed from mold (top left corner removed for analysis) (b) Under bending (c) Load on concave side by 4dram glass vial and forceps (d) loaded from concave direction with forceps

4.4 Carbon Nanofiber Composites

Composites are a popular option for combining material properties, such as light weight and high strength, that are uncommon or more expensive when found in a single material. A composite is composed of a matrix material and a reinforcement material. Although the composite materials may be significantly different from each other (polymer-glass, i.e. fiberglass composites), they can also be quite similar (e.g. carbon-carbon composites). In this section the use of carbon nanofibers as both the reinforcement material and as the matrix material are presented. As the reinforcement material, the focus is for incorporation in a fiber reinforced polymer (FRP). As the composite matrix,

focus is given the incorporation of glass fibers into a fibrous carbon foam. However, as either the matrix or reinforcement, many choices for material combinations exist.

4.4.1 Carbon Nanofibers as the Composite Reinforcement

Based on the results discussed for general carbon deposition (Section 4.2) a variety of morphologies can be achieved. The fiber structure will have a direct impact not only on the properties of the fiber itself, but on how load is transferred between the matrix and nanofiber. By exploiting the physical structure of the carbon nanofibers it is possible that the interfacial shear strength can be sufficient as to not require a chemical treatment for adequate bonding between the fiber and the matrix. Alternatively, this method could be used in conjunction with chemical bonding means to enhance interfacial shear strength. Three general morphological considerations are made specifically for this purpose; size control, surface roughness, and helicity.

4.4.1.1 Impact of Fiber Diameter

Nanofiber diameter is the most basic parameter and simplest to control. It is also perhaps the most important quality to achieving desired composite properties. Typically a fiber will be equally sized with the catalyst particle from which it is generated,[17,18,41] but when catalyzing carbon nanofibers from large particles (>500nm) it is more difficult to predict resulting fiber size since fractionation of the particles tends to produce inconsistent fiber sizes. Thus, controlling catalyst particle size is the key to controlling fiber diameter and consequently composite properties.

However, in this study the endeavor has been to show that other, easily controlled factors can also impact diameter. For example, we found that gross gas flow rate over the catalysts particles had a remarkable impact. In Figure 39a which is representative of a typical fiber yield at 15sccm each of oxygen and ethylene (1:1) at 550ºC fiber diameter is varied and significantly larger than when grown at 100sccm each of oxygen and ethylene (Figure 39b), even where the temperature and reactant ratio remained the same.

a) 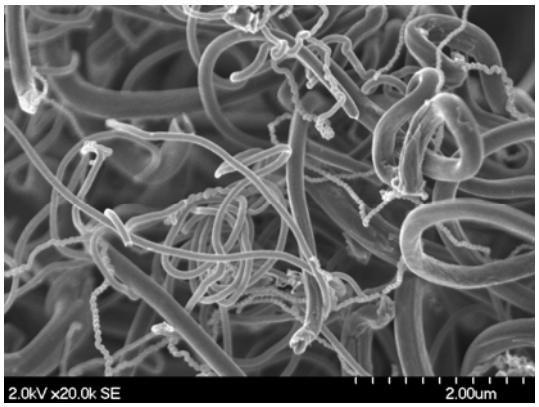

b) 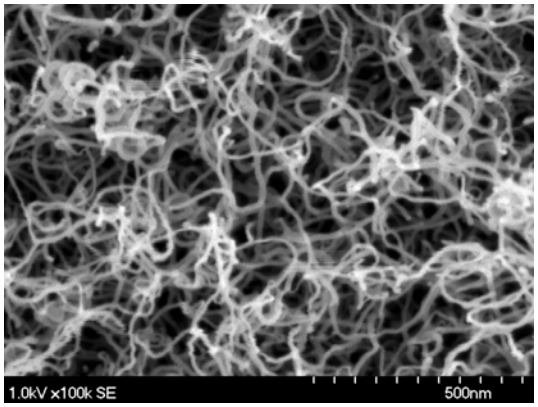

Figure 39 - a) SEM image of CNFs grown in 15sccm C2H4 and O2 (1:1) at 550ºC (20,000X magnification) and b) CNFs grown in 100sccm C2H4 and O2 (1:1) at 550ºC (100,000X magnification)

This method of reducing the fiber size was successful with indifference to the catalyst size. Controlling the diameter and the variation in diameter is important for individual fiber properties and also overall composite properties as greater uniformity in the fibers will yield greater predictability in the composite.

4.4.1.2 Impact of Fiber Helicity

Another interesting fiber trait that can be consistently reproduced is the helicity, or degree of twist, along its longitudinal axis. Variations in the cross-sectional area of a nanofiber, that are capable of being penetrated by the matrix material, are a path to better load transfer between the matrix and nanofibers. Even if interfacial bonding is compromised, the physical interference (mechanical interlocking) of the nanofiber with the matrix could restrict nanofiber pullout. This occurs when the larger cross sections of the fibers encounter the smaller cavities of matrix material, created by the smaller cross sections of the fiber, during pullout.

The manner with which the cross section varies will also play a role in how the nanofibers distribute the load pre and post pullout. Random variations in the cross sectional diameter would create areas of high and low stress along the length of the nanofiber, while a periodically varying diameters would help to more evenly transfer the

load along the length of the nanofiber. Commonly, helical nanofibers of periodically varying diameters are created in this process. One such example is shown in Figure 40.

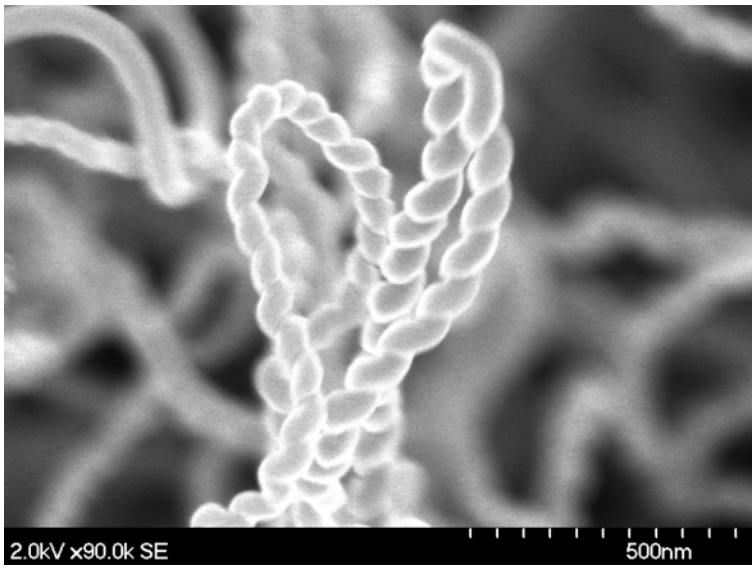

Figure 40 - Twisted fiber morphology common at temperatures above 600ºC (90,000X magnification)

There are various methods for producing helical fibers, but typically include the use of alloys [46] or other non-metallic additives.[18] In this work, only pure Pd particles were used. Helical nanofiber morphology was typical for Pd catalyzed carbon at elevated temperatures (i.e. above 600ºC). The fibers diameters are typically less than 100nm, but again are a function of flow as described in the preceding section.

4.4.1.3 Impact of Fiber Roughness

The last fiber morphology presented is that concerning surface roughness. Similar to the helical fibers, a rough surface will increase the frictional resistance to sliding and hence, the interfacial shear strength will see a concomitant rise. Indeed, this particular case has been shown to cause an increase in initial sliding stress.[47] To achieve a roughened surface architecture the gas ratio was reduced from 1:1 to 1:2 (ethylene to oxygen) at a temperature of 550ºC as in other cases. The morphology of the fibers is shown in Figure 41.

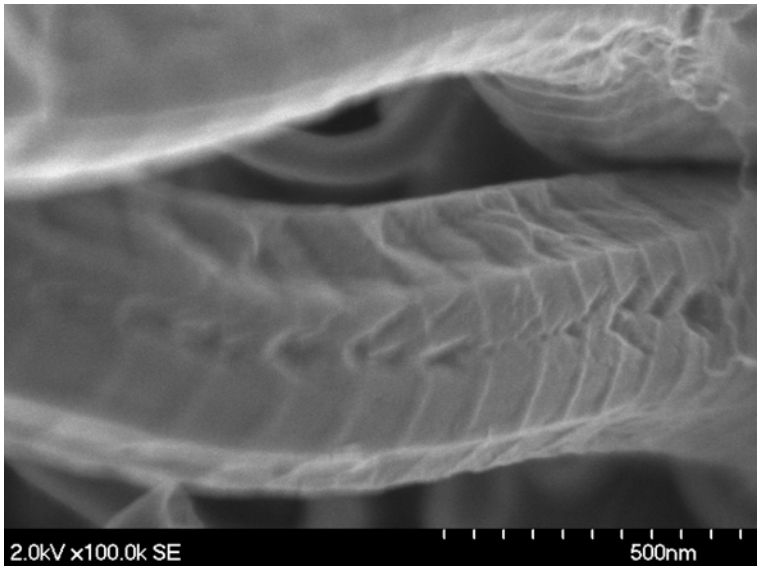

Figure 41 - Enhanced surface roughness on CNFs produced in a 1:2 (ethlyene:oxygen) environment (100,000X magnification)

4.4.2 Fibrous Carbon Foam as the Composite Matrix

The process for creating fibrous carbon foam (Section 3.2.4) allows for the inclusion of a variety of different reinforcement materials. Because the process does not need to exceed 550 ºC, materials with relatively low melting temperatures (e.g. copper) can be added before the growth process is initiated. As the fibers grow, they encase the added material, locking it into the foam structure. An example of this is shown in Figure 42. Here, glass fibers were added to the mold with the palladium powder, and then processed to create the foam/fiber composite. The cross section was created by simply cutting through the foam with scissors.

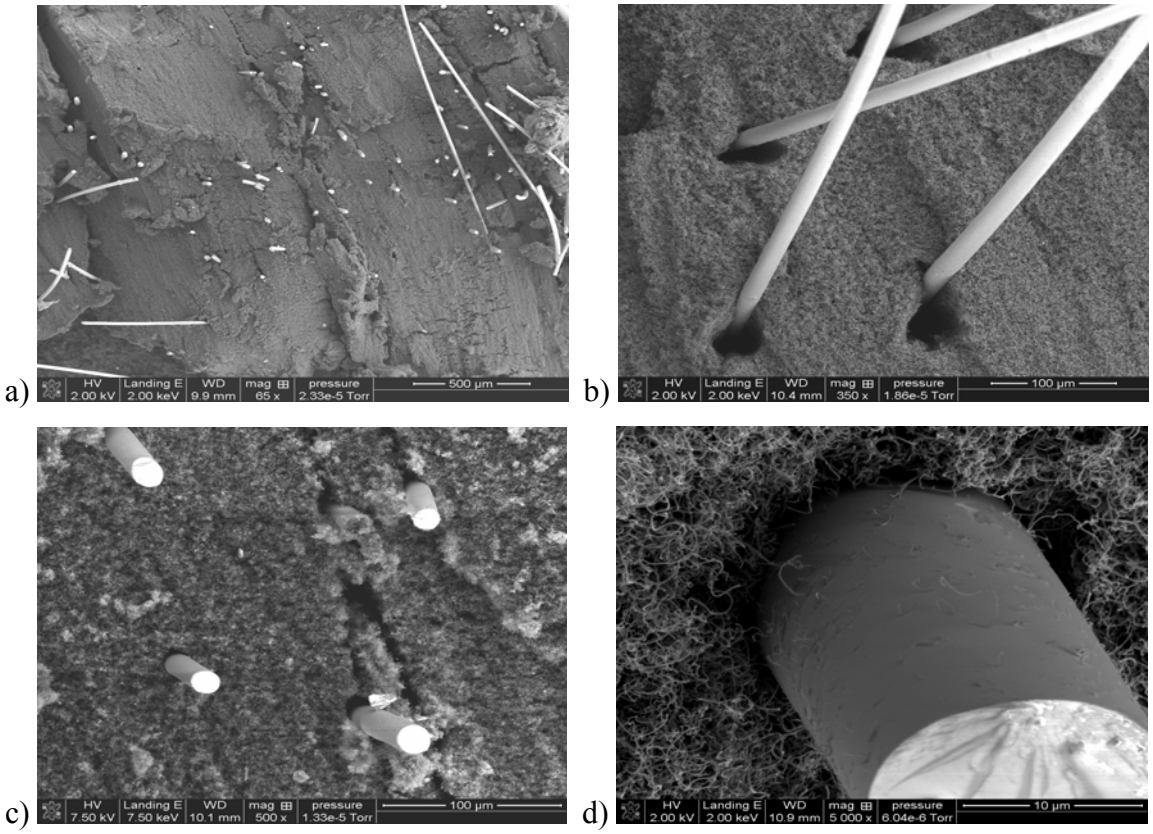

Figure 42 - Fibrous carbon foam with glass fibers as reinforcement at magnifications of (a) 65X, (b) 350X, (c) 500X, and (d) 5,000X

Although fibers are perhaps the most common method for reinforcement, other material forms such as metal mesh, particles, tubes, etc. may also be integrated by this approach.

5 Discussion

The results of this investigation will now be discussed in regard to the importance, implications, and usefulness of the findings. As in the previous chapter, the discussion will be divided into sections on carbon deposition in ethylene-oxygen mixtures, ethylene-hydrogen mixtures, and the applications of the carbon nanofibers generated by these methods. Since palladium in ethylene produced negligible carbon deposition, it will not be included in the discussion.

5.1 Deposition in Ethylene-Oxygen Mixtures

Although rarely used for low temperature carbon deposition, palladium has been found to work remarkably well in a partial combustion environment. Not only did carbon formation begin quickly, after commencement it was extensive in both growth rate and particle longevity. Large deposits formed quickly and no definite limit was found for amount of growth achievable within practical time constraints (<24hrs).

This study provides information on two topics of importance to fully understanding carbon growth from metal catalyzed reactions with hydrocarbons at elevated temperatures. First, the data provides new phenomenological information, including the influence of factors not typically explored, such as the form of the metal template. Second, this data contributes to a better understanding of the mechanism of carbon deposition in a reaction mixture (combustion) environment, rather than from reducing environments.

It was observed that low temperature deposition of carbon by Pd from ethylene is only feasible with the addition of oxygen to create a partial combustion environment. This was convincingly demonstrated by the fact that negligible carbon growth was observed on palladium templates exposed to ethylene, in the absence of oxygen, at 550°C even after 24 hours. In contrast, remarkably high net carbon growth rates were observed at 550°C in the presence of a fuel rich mix of oxygen and ethylene after even 5min.

The morphology and rate of carbon deposition is closely associated to the structure of the metal, temperature, and position in the reactor. This is illustrated by the occurrence of planar carbon films forming on Pd foil, whereas under identical conditions (in some cases side-by-side) filaments grew on particles and sputtered films. Exclusive to Pd foil, after extended periods of growth (>30min depending on conditions), a mix of planar and filamentous carbon was observed. The clear differences in structure suggest a difference in mechanism.

Also, influencing growth characteristics is the position in the reactor. Unfortunately, the two main factors, temperature and position within the reactor, are somewhat convoluted. The data indicates that both factors influence the nature and rate of growth. As noted earlier, there are instances of no growth and rapid growth at the same temperature, but at different reactor positions. Moreover, it is quite clear that there are positions of remarkably high growth rate that do not correspond precisely to temperature, or local carbon concentration. Also, in the same reactor, but at different positions, the morphology of fiber structures, in particular, is dramatically different (e.g. diameter and helicity).

Furthermore, the carbon deposited on Pd by this method is poorly crystalline. In earlier studies of growth from fuel rich ethylene/oxygen mixtures, using platinum or nickel, the carbon was found to be graphitic.[9,10] In this case, in which Pd was the catalyst, there is absolutely no indication of graphitic structures forming. In all cases, on all templates, the structures are best described as a mixture of amorphous, and turbostratic carbon. Because of this universal result it seems crystallinity is not practical for the conditions reported here. However, as reported for "stacked cup" carbon nanofibers,[48] graphitizing at high temperature may present a means of increasing the crystallinity, but that would create an additional step at a temperature significantly higher than the initial production requires, hence complicating a rather simple, low temperature process.

For establishing crystallinity in carbon nanostructures, using multiple methods gave insight to the strengths and weaknesses of each technique. For their simplicity and lack of

ambiguity, it seems TEM and XRD analysis are the most useful for determining crystallinity. Both methods give direct indication of crystallinity whereas Raman and TPO are typically based on contrasts between samples. In many cases, TEM has the added benefit of electron diffraction techniques for establishing crystal properties, but because TEM covers such a small area of a sample it cannot necessarily be directly correlated with the overall structure as local variation may exist. XRD gives a good indication of overall crystallinity, but does not provide much information about the morphology of the fibers. TEM and XRD compliment each other well, and they provide the most complete picture for the effort.

Finally, we consider the implications of the data for the mechanism. In brief, all data is consistent with an earlier proposed mechanism of carbon structure growth in a combustion environment.[9] That proposition is that growth occurs not via the thermal decomposition of hydrocarbon molecules, but rather by the decomposition of carbon containing radicals created in a combustion process. This mechanism is consistent with several observations: (i) the dependence of growth on position within the reactor, (ii) the dependence on temperature, and (iii) significant carbon growth on palladium using ethylene as the carbon feedstock is only observed in reaction mixtures.

Regarding the dependence on position, if thermal decomposition were the mode of carbon generation, there would be a monotonic decrease in deposition rate on position. That is because both combustion processes and carbon deposition processes would decrease the ethylene concentration monotonically and hence, the deposition rate would as well. It is impossible to interpret the data as showing a monotonic decrease in deposition rate with position. The measured dependence on temperature is also not consistent with a thermal decomposition model. Indeed, no growth at all is observed at the highest temperatures reached in the study. As thermal decomposition rates increase with temperature, there should be a monotonic increase in rate with temperature, not a change to a zero rate above some arbitrary temperature. Finally, the fact that a reaction mixture is required to observe any appreciable growth is also inconsistent with a thermal decomposition model. In contrast, the dependence of rate and morphology on residence

time is consistent with a deposition-from-radicals model. Indeed, in an ethylene "flame" many dozens of radicals are present, and the concentrations of particular radicals will vary dramatically with residence time. Thus, if one particular radical is responsible for most of the growth, an optimum spot (area of high concentration) would be anticipated. Different morphologies can be attributed to different radicals. Therefore, several optimum spots are anticipated throughout the length of the reactor for one set of growth parameters, possibly each with its own morphology.

It is valuable to note differences and similarities of observation with earlier work. For example, the fact that deposition in reaction mixtures occurs only over a limited temperature window was observed previously with both platinum [16] and nickel [9] catalysts templates. In this case the low temperature is nearly 100°C lower than that previously reported. However, in earlier studies deposition was only studied at a single reactor position. A more thorough study may have yielded the same temperature window as observed in this work.

5.2 Deposition in Ethylene-Hydrogen Mixtures

Four findings of the ethylene-hydrogen results necessitate a detailed discussion, particularly as they relate to the mechanism of growth of planar carbon structures. First, the structure of the Pd metal impacted the morphology of the carbon structures that grew from ethylene-hydrogen mixtures. Second, growth was negligible without hydrogen. Third, the growth only took part over a limited temperature range, and growth rate is strongly dependent on temperature. Fourth, the growth of planar carbon structures is far slower than that of fiber structures.

It is instructive to compare the above findings with observations made for carbon structure growth from combustion mixtures. The first finding is similar to that observed in studies of carbon deposition from fuel rich ethylene-oxygen mixtures. Once again, on larger metal structures (e.g. foil), planar carbon formed, and the structures were turbostratic rather than graphitic. Also, on smaller forms (e.g. nanopowder) fibers

formed. In both cases the fibers were not well crystallized, and crystallinity was found to change proportionally with temperature.

Second, it was again notable that growth only occurs in gas mixtures capable of creating radicals. Indeed, it was long ago established that ethylene and hydrogen will react homogeneously to form higher hydrocarbons,[49] and in the presence of palladium catalysts, hydrogenation occurs even at 0°C,[50] probably because of the formation of hydrogen atoms on the palladium surface and subsequent reactions between hydrogen atoms and the hydrocarbon.[51,52] At higher temperatures (ca. >350°C) it is known that palladium and other noble metals will create H atoms capable of traveling relatively far through the gas phase to effect reactions.[53] Thus, the well known homogeneous reactions between ethylene and hydrogen[54] and between ethylene and H atoms[55] are likely to be significant at the temperatures at which carbon growth was observed in the present study.

This second observation also inevitably leads to the question of the role of hydrogen in the mechanism of fiber growth. Several other studies, also observing the impact of adding hydrogen on rate and nature of fiber growth present a host of explanations. Most of the literature discussing the impact of hydrogen pertains to Pt, Fe, Co, and Ni catalysts. On these metals the postulated effect of hydrogen includes (i) aiding metal surface reconstruction,[12,15,18] (ii) improving catalytic activity, and enhancing catalyst life,[11,13,15,18,29,56] (iii) helping generate favorable species for dissolution into the metal catalyst which provides a ready supply of carbon for subsequent precipitation,[15,21] and (iv) improving fiber crystallinity.[13,29]

Park et al. found that adding hydrogen increases the rate of solid carbon production and fiber crystallinity for iron-nickel catalysts.[13,29] Both rate and crystallinity were also found to depend on the iron-nickel ratio as well as the carbon feedstock (i.e. ethylene or carbon monoxide). They also found that using only hydrogen resulted in the hydrogasification (weight loss) of solid carbon.

Rodriguez postulated hydrogen may serve two purposes. The first is that hydrogen chemisorbed over the surface prevents condensation reactions leading to the formation of graphitic overlayers.[18] Second, hydrogen adsorbed over metals weakens the metal–metal bond leading to an induced mobility of surface atoms known as faceting or reconstruction.[11,18]

Owens et al. [15] made an intriguing and unique suggestion regarding the role of hydrogen in platinum catalyzed filament growth, where hydrogen was found to be a necessary ingredient for filament growth. They suggest that hydrogen changes the chemistry of the hydrocarbon at the metal catalyst surface. It does this by dissociation of hydrocarbons on the metal catalyst surface in both ethylene and acetylene, and by hydrogenation of ethylene to ethane. The fraction of input hydrocarbon converted to solid carbon increases as hydrogen concentration increases (tested to 80% hydrogen). The impact of hydrogen was observed to be more pronounced with acetylene than ethylene. Both of these observations are consistent with the suggestion that hydrogen is an active chemical agent helping create carbon radicals. This group also suggested hydrogen disrupts the surface graphite formation which deactivates the catalyst (occurring at virtually monolayer coverage). Additionally, they suggest that hydrogen's role is not simply to maintain a clean surface, but to induce reconstruction of the platinum.

Yoon et al.,[56] whilst using acetylene with cobalt particles, state that hydrogen serves to dilute the acetylene and cleans the surface. Also, hydrogen is important to maintain optimum carbon concentration in the catalyst, and without hydrogen, growth rate decreased with increasing acetylene flow, possibly because of excess carbon on the catalyst surface.

It is also clear that hydrogen does not always greatly impact the deposited carbon. For cobalt-copper catalyzed carbon nanofibers, Chambers et al.[14] noted a minor increase in catalytic activity at hydrogen concentrations up to about 2%, and a decrease of activity at higher concentrations. For pure cobalt the addition of hydrogen was not found to influence the carbon deposition characteristics.

Although palladium is not commonly employed for catalyzing carbon nanofiber growth, the palladium-hydrogen system is well-studied.[57] Palladium's affinity for hydrogen is expected to be vital in governing the resulting carbon deposition since not only is hydrogen absorbed into the bulk, but various forms of activated hydrogen are bound to the surface, and geometric and electronic changes are induced by the adsorbed hydrogen which effect its catalytic properties.[8]

The above literature review clearly shows the role of hydrogen in carbon deposition structures is not clear, particularly for planar carbon structures such as those found on foils and around encapsulated particles. The evidence produced herein and the observations of other groups are consistent with the suggestion that hydrogen plays an important role in creating radical species containing carbon atoms. For example, atomic hydrogen and active carbon species have been found critical for catalytically grown, single-walled carbon nanotubes.[58] Indeed, some of the other suggestions, for example that hydrogen cleans or even reconstructs the catalyst, seem implausible for a planar growth mechanism. How can hydrogen clean the surface of a fully encapsulated catalyst surface? In a radical species model, by contrast, the source of carbon atoms, radicals, can be produced homogeneously, such that free surfaces of the catalytic metal are not required.

The generation of radicals may also take place heterogeneously. It is well known that palladium is an excellent catalyst for the decomposition of hydrogen molecules to from hydrogen atoms.[51,52] For heterogeneous radical generation, palladium would be effective through the dehydrogenation of ethylene, but carbonaceous deposits have also been found to interact with gaseous molecules by hydrogen transfer reactions due to high hydrogen concentrations in the adsorbed carbon.[59] Although carbonaceous deposits are primarily attributed with poisoning catalytic metals, they also strongly influence the active catalytic behavior.[60] Frenklach and Ping have proposed that by surface migration along the edge of a graphene sheet a five member ring may become incorporated by conversion into a six member ring, and that the process is mediated by gaseous hydrogen atoms.[61] It is evident that the activity of deposited carbon should not be considered inconsequential.

The third result, that growth rate and type is temperature mediated, is also qualitatively consistent with that observed in ethylene-oxygen mixtures. For growth from both combustion mixtures and from ethylene-hydrogen, there is a peak in rate as a function of temperature. However the growth curves are temperature shifted in the two cases. For all catalyst templates the maximum growth temperature in ethylene-hydrogen mixtures is significantly higher than it is in combustion mixtures. For example, maximum growth rate, on average, for palladium in an ethylene-oxygen mixture is about 550°C, and no growth is observed at 700°C. In contrast, in ethylene-hydrogen mixtures, most templates yielded the greatest carbon deposition at 700°C, where combustion mixtures were ineffective.

This strong temperature dependence on rate and growth type can be explained by a concomitant change in radical type and concentration with change in temperature. There is a great deal of evidence that radical-based chemical processes are only found to occur over a limited temperature range.[62,63] Hence, the radical hypothesis is consistent with a general empiricism of radical-based chemistry. Also, the particular gas chemistry will impact the range over which radicals form. There is every reason to suspect that radical formation in combustion mixtures will have a different temperature profile than observed in non-combustion mixtures.

The fourth observation, that planar structures grow much slower than nanofibers, is consistent with combustion mixtures as well. The growth of fibers is relatively easy to explain. It has been repeatedly demonstrated that particles of certain metals are able to catalyze the growth of fibers via a process of carbon adsorption at the metal/gas interface, followed by diffusion of the carbon through the particle, and finally precipitation at the metal/fiber interface.[17-21] This diffusion model appears to be a suitable explanation for fiber growth encountered herein. However, as noted in earlier publications,[9,64,65] the observations regarding planar carbon indicate the fiber growth mechanism cannot be readily adapted to explain the mechanism of growth. For example, once the templates are encapsulated, how does the metal continue to exert a catalytic influence?

It has been suggested that in the case of encapsulating carbon growth, some of the catalytic metal is transported to the surface by diffusion through the encapsulating carbon in an atomically dispersed form,[25] and this catalyzes the growth of additional layers of carbon. No direct evidence for the existence of atomically dispersed Pd was found, and it seems the dispersed atoms would be thermodynamically unstable and form clusters of atoms. The results of the general deposition reactions makes it quite clear that small clusters, or particles of Pd catalyze *filament* growth, not the growth of planar carbon structures.

Although the data is not sufficient to draw a strong conclusion, we continue to maintain that the most likely mechanism of continued growth *after* catalyst encapsulation is the catalytic nature of carbon itself. Specifically, it is reasonable to postulate that graphite, or small, ordered regions of carbon, self-catalyze further growth from carbon fragments/radicals, produced via homogeneous or heterogeneous reaction processes. In other words, the carbon atoms are created on the carbon surface via the decomposition of parent radicals. These atoms diffuse on the surface until bonding strongly at an edge site, possibly decomposing to release fragments (e.g. H atoms or molecules) thus extending the graphite structure, turbostratic or otherwise. This self-catalytic behavior has been observed from multi-walled carbon nanotubes which adsorb and incorporate C_n species at edge sites to increase in both length and diameter.[66]

Venkateswaran et al. studied the duality of carbon as both a catalyst and an inhibitor,[67] and found that very thin films of carbon (less than monolayer coverage) act to inhibit the decomposition rate of methane, and thicker films (>30nm) acted to significantly increase the rate while also depositing additional layers of carbon without losing catalytic activity. This agrees with the increase in growth rate with time for foils if initial growth is slow due to the inhibitive effects of disperse carbon, and after eventually gaining a thick enough layer that a self-catalyzed reaction could begin the rate then increases.

That growth rates of planar structures are much slower than that of fibers, is consistent with a mechanism by which carbon self-catalyzes further carbon deposition. It is also

notable that fibers will grow at temperatures (e.g. 550°C) at which barely any planar carbon growth is observed. In particular, the much slower growth rate of planar structures is evidence that a different mechanism is at work. If carbon is acting to catalyze solid carbon, it would be expected to be significantly slower based on the relative effectiveness in comparison to palladium. This is strong supporting evidence that the mechanism of fiber growth and the mechanism of planar structure growth are not the same, and that a carbon self-catalysis method may help to explain the differences.

5.3 Carbon Nanofibers Applications

Advancement of materials can lead to new products, or can improve existing ones. For example, carbon fiber reinforced polymers are used extensively in applications requiring lightweight and high strength (e.g. aerospace). The fibers used in the traditional composites are typically generated by the pyrolysis of polyacrylonitrile (PAN), [68] but the superior properties of carbon nanotubes are driving research on using them as a replacement for the traditional carbon fibers in advanced composites,[69] and carbon nanofibers are also being investigated for composite applications.[70] The applications of carbon nanofibers explored in this work are limited to composite and carbon foam potential, although other applications exist.[18,41] More specifically, their potential as polymer reinforcement, and their use as a fibrous carbon foam with and without secondary fiber (i.e. glass fibers) reinforcement is discussed.

5.3.1 Carbon Nanofibers as a Composite Reinforcement

There are many choices for generating carbon nanofibers, and Pd catalyzed generation demonstrates some key characteristics that are useful for reinforcement of composites. Some of the benefits of palladium are that it grows fibers quickly (>1μm/min), sustains that growth for as long as tested (~24hrs), and the resulting morphology can be controlled as a function of reactant gas ratio, flow rates, and temperature. The use of a combustion environment for growth also has advantages. The reactant gases used here are common and inexpensive, and require no special handling as

some other gas types (e.g. acetylene), relatively low temperatures can be employed and growth rates are remarkable.

Also of importance is the robustness of the Pd catalyzed carbon nanofiber growth. As found in the general deposition study, the temperature window for growth extends from below 350ºC to above 650ºC. This wide range, especially the lower temperatures, could be useful for incorporation of nanofiber onto traditional carbon fibers. As found by Downs et al.,[71] the addition of carbon nanofibers to the surface of carbon fibers yielded an improvement of nearly five times the interfacial shear strength. Low temperature processing of Pd CNFs with these tunable properties could act to improve this number even more without damage to the parent fiber more likely at higher temperatures.

A major roadblock that is not addressed through morphology is that of uniform dispersion in the matrix. This common hurdle may be overcome through the functionalization of the fiber surface. This has been shown to work well with both carbon nanotubes and nanofibers.[72,73] Since even a well-controlled morphology will not serve to benefit the composite if agglomeration occurs, it reasons that it would be important to consider functionalization. The shape and texture of the previously discussed nanofibers is not to replace current methods of interfacial strengthening but rather to supplement them and provide an improved overall product by the tuning of small scale features.

5.3.2 Fibrous Carbon Foams

A variety of technologies for the generation of carbon foams exist. Current processes rely on some precursor whether it be an existing polymer foam,[74-78] sacrificial template,[79,80] or carbonaceous material such as pitch.[81-85] However, none of these methods appear to be simpler or less costly than the process described in Section 3.2.4. Also, the flexibility of the reported process enables a variety of foams to be created without further processing steps. To evaluate the usefulness of growing fibrous carbon foams (FCFs) it is beneficial to compare it to the foaming processes mentioned previously.

The first method of creating carbon foams to be discussed relies on the use of polymer foam to be a sacrificial template. The template foam used can be a thermosetting polymer,[74] or a stabilized thermoplastic polymer such as polyurethane.[76,77] The stabilization typically consists of the impregnation of a thermosetting material which helps retain the shape of the original foam. An example of this process with rigid polyurethane of the polyester-type consists of curing, oxidizing, and pyrolyzing steps.[75] Curing time and temperature will depend on the polymer used in order to produce sufficient cross-linking, but the preferred temperature is from 150-250°C for a period of 8-24hr. Oxidation is done at 200-255°C in air to bring about a weight loss as needed to ensure the foam does not melt or distort. Depending on the temperature, reaching the desired minimum weight loss of 3.6% will take from 1-30hr., decreasing in length with an increase in temperature. Pyrolysis, or carbonization, is done at 900°C, being raised to that temperature at a rate of 50°C/hr.

Thermosetting foams reduce the need for stabilization as described above. Ford,[74] describes a process in which the polymer foam is heated to ~260°C in 30min and held for one hour, followed by an increase to ~1200°C in 5hr, allowed to soak for 1hr and then allowed to cool. By starting with a thermosetting polymer the complexity can be significantly reduced, and the reticulated vitreous carbon (RVC) foams created by this method have many applications.[86]

The second method uses template synthesis to create porous carbon. In general, the process involves a porous inorganic template into which carbon is introduced, typically as a polymerizable organic material. The organic material is then polymerized and pyrolyzed to carbon. The template is then removed by dissolution or evaporation.[87] This method allows for creating a precise pore size and shape which allows for specific characteristics and applications.[79,80] The inorganic template is commonly silica, but other materials are may be employed, and the sacrificial material can be quite complex to generate itself. Furthermore, removal of the template may require hazardous chemicals such as hydrofluoric acid, as in the case of silica.

The final method described here enlists the use of pitch-based precursors for making carbon foams. This method is the most common, and has multiple variations for accomplishing the foaming. Perhaps the most well-known is the process developed at Oak Ridge National Laboratories (ORNL).[81] In this process, pitch is introduced into a mold which is then purged of air by evacuation or filled with an inert gas. The pitch is then heated and coalesces into a liquid at ~50-100°C above the softening point. The pressure is then raised (by inert fluid) to a static pressure of ~1000psi. The pitch is then heated to a temperature at which gases begin to evolve and foam the pitch, followed by a rise in temperature at which the pitch cokes. The pressure and temperature are then lowered gradually. An example of the process[88] with Mitsubishi ARA24 mesophase pitch includes heating to 300°C under vacuum (<1 torr), followed by back-filling and pressurizing to 1000psi in nitrogen. The temperature is then raised to 800°C at a rate of 2-5°C/min and held for 15min. The foam is then cooled to room temperature at a rate ~1.5°C with a pressure release rate of ~2psi/min to atmospheric. The foam is then heated to 1050°C for carbonization.

A similar approach may utilized at lower pressures (0.5-1.5 atm) by heating the precursor (coal, coal extracts, or pitches) to remove volatiles followed by cooling and powdering, then foaming in an inert environment.[89] In the case of bituminous coal, the reactor is heated to 385°C at a rate of 2°C/min in nitrogen and allowed to soak for 2 hr. After cooling to room temperature, the product is ground into a fine powder and placed back in the reactor and heated to 500°C at 2°C/min. and held for 2hr in stagnant nitrogen.

An atmospheric pressure method[82] involves heating a petroleum-derived mesophase pitch to 460°C and holding for 0.5hr before cooling. The foams are then oxidized up to 350°C at a rate of 0.05°C/min. The oxidized foams are then carbonized at 1000°C for 1hr in nitrogen.

Although, there are still more methods of creating carbon foams, the general trends become apparent with the listed processes. These processes generally require carbon precursors (pitch, coal, etc.) which must be processed, high temperatures, and/or high

pressures. Even though the precursor may be inexpensive, the process may be quite complex. A process[90] developed at West Virginia University (WVU) uses coal as a precursor which is quite cost effective, but the process involves de-ashing and then coking the coal which potentially requires very high pressures (15-15,000psig with 50-1000psig preferred), as well as carbonization at ~1000°C, and several other steps including chemical treatments.

So it seems not only the cost of the precursor, but also the cost and simplicity of the process must be considered. Although catalytic metal powders are certainly more expensive per gram than pitch for example, the amount of catalyst used is small relative to the carbon output. In the provided example for creating fibrous carbon foam (Section 3.2.4), 5mg of palladium powder catalyzed >400mg of carbon growth in under 19hr, a time comparable to the listed methods when considering carbonization and slow temperature programs not needed for fibrous carbon foams. The 8000% weight gain demonstrated in the given example can be further increased by decreasing amount of catalyst and increasing time to allow for greater fiber growth before the mold becomes blocked. As noted, by increasing the amount of catalyst, the mold could be filled in a few hours. However, the foam produced in this manner tended to have less structural integrity than when formed with less catalyst for a longer time.

Using less catalyst is also advantageous for obtaining higher purity carbon foam without subsequent demineralization. If desired, the metal catalyst can be removed from the fiber using an acid treatment appropriate for the metal. The carbon fibers themselves are not impacted by ordinary acid treatments. However, leaving metal catalysts in foam is not uncommon in many other foam generating technologies. Indeed, for urethane foams[91] (the yellow foam found in furniture, packing, etc.) the metal complex catalyst material used to grow the foam (often tin[92]) is generally still found in the foam, and constitutes on the order of 5% by weight. In our samples the metal content by weight is generally less than 3%.

It is clear that the properties of the foam produced including stiffness, electrical and thermal conductivity, resistance to burning, pore size and uniformity, etc. are a function of the process employed. Hence, comparison based only on the complexity, duration and/or cost of the production technique is not sufficient. In reality, the selection of a particular foam intended for a targeted application is more likely to reflect the properties of the foam than its cost. The ability of a particular foam to fulfill the assignment is the main criteria for selection. This suggests that a foam generation procedure with the flexibility to produce a variety of foam morphologies as well as the ability to incorporate materials to create composites with an even wider range of properties might be generally preferred. A low temperature process as described above, that can produce foams based on catalyst identity and load, temperature program, and gas ratio offers a simple and quick method of meeting specific requirements.

In these FCFs the properties of the fibers control the properties of the foam, and there are many characteristics of carbon nanofibers that are attractive for advanced technology. This method of molding carbon nanofibers to create a dense and stable collection of them provides a means to implement their use in applications such as hydrogen storage, and as a catalytic support.[18,41]

As with all of the reviewed methods, the final foam structure must be graphitized to be highly conductive. This step has been found to be very rate sensitive due to the propensity for microcracking with reduces electrical and thermal conductivity.[81] It is believed that fibrous carbon foam will not be as sensitive to microcracking during rapid cooling and heating as other carbon foams are,[78,81,83] because the fibers are not rigidly interconnected and can expand and contract without appreciable impedance. Therefore, it is likely fibrous carbon foams may be raised more quickly to traditional graphitizing temperatures,[48] but it has also been found that some carbon nanofibers gain appreciable crystallinity at temperatures as low as 1000°C.[93]

The nearest carbon foam process to that described here is the use of carbon nanotubes (CNTs) to form carbon foams.[94] The process involves an extremely compact nanotube

array, or wetting and subsequent evaporation to form a pattern in the array. Aside from using a carbon nanomaterial, this process is significantly different in execution. The CNT foam would have the advantage of the properties of the CNTs, but in simplicity and applicability it seems the less exotic fibers produced by the FCF process are, on balance, a more practical solution to incorporating nanoscale properties with macroscale convenience.

Relative to the existing technologies, one of the major advantages to the FCF process is the ease of incorporation of other materials. Moreover, our method allows for more flexibility of composition. Indeed, as the temperatures involved are relatively low, a wide variety of materials can be incorporated. Aluminum, copper, bronze, or other materials with a melting temperature below 1000°C can all be incorporated using the FCF process, but not into carbon foams that require carbonization or graphitization which require temperatures at or above this. Also, since fibrous foam is created as the matrix *in situ*, the reinforcement is integrated during the "foaming" process, and this eliminates latter steps and saves time.

One of the most recent examples for making a carbon foam composite activated carbon/carbon composite is given in a patent application by Jing Wang.[95] An example of the process requires mixing and blending a specially prepared polyimide powder with carbon fibers or other materials, compression to 5,500 psi (>400 atm) and heating to 800°C under inert gas for several hours. This is also a "one pot" approach in which the matrix and reinforcement are integrated before the foaming process. The need for relatively high temperature will limit the materials that can be incorporated.

Similar to the pervious method, a method of reinforcing coal-derived carbon foams (WVU method) includes the addition of the reinforcing material in either the dry (powder) state, or after solvent addition. However, the reinforcement materials are preferably carbon based (e.g. carbon nanotubes or nanofiber, coke.)

Generation of pitch-based carbon foam composites by the ORNL method is reported[96] for a carbon foam core with carbon fiber or carbon-carbon facesheets. Also, epoxy impregnation of the carbon foam was used to create a carbon polymer composite. No method for inclusion of fibers, particles, etc. is mentioned with this process, but because the process is identical to generate the foam, the incorporation of low melting temperature materials would be unfeasible.

Because of the simplicity and flexibility of the FCF process, it seems a viable option for generating commercially attractive carbon foam. Although the properties need to be further explored before the exact niche it may fit is discovered, the potential to serve many industries is apparent. Because these foams, in their "pure" state have the benefit of exhibiting properties based on the individual nanofibers as well as their collective properties (e.g. porosity), the variety of uses is expected to be vast. Being able to incorporate other materials, or incorporating the foam into other materials, is equally valuable and important to identifying the applications.

6 Conclusions

It has been demonstrated that palladium can be an exceptional catalyst toward the deposition of solid carbon from ethylene in two distinct forms: nanofibers and thins films. Four forms of palladium were tested: sputtered film, foil, sub-micron powder, and nanopowder. The deposition of carbon can be achieved by a very simple method. In this method ethylene and oxygen or hydrogen are flowed through a single-zone, horizontal tube furnace at atmospheric pressure and temperatures from 550-700°C. Other temperatures were found to result in carbon deposition, but maximum deposition rates occurred between the aforementioned temperatures. The addition of a secondary gas such as oxygen or hydrogen is vital in driving the deposition. Although both gases improve deposition, the manner in which they do differs. Ethylene-oxygen mixtures are preferred at lower temperatures (i.e. 550°C) than ethylene-hydrogen mixtures (i.e. 700°C). Pd sub-micron was the most prolific form of palladium at producing solid carbon in a combustion environment, whereas nanopowder was in ethylene-hydrogen mixtures. Palladium, of any form, did not catalyze appreciable carbon deposition at any temperature in ethylene alone. These findings suggest that radical species may be imperative to inciting carbon deposition, and since fibers and thin films of carbon are very different structures, a different mechanism for growth is expected, and the role of carbon as a catalyst is suggested to be important in catalyzing further carbon deposition.

The resulting carbon deposition rate and morphology were found to be a function of temperature, position in the reactor, duration of the reaction, gaseous environment, and form of palladium. These factors were all interconnected, and had to be considered collectively to predict the efficacy of the reaction toward solid carbon production. Crystallinity was found to increase with temperature, and ethylene-hydrogen mixtures produced more crystalline structures than were formed in a combustion environment, however the carbon produced under any conditions tested here was never fully graphitic, and instead was turbostratic or nearly amorphous.

Based on the findings of the general catalysis study, the promise of application for the carbon nanofibers was anticipated and demonstrated through the formation of fibrous carbon foams. These foams can be generated using a small quantity of palladium (<5% carbon output by mass), and both the macro- and microscale properties will define the overall properties, and therefore the projected use. These fibrous carbon foams can be combined with other materials to form composites which can be integrated during the formation of the foam. Because the foam process does not require high temperatures, a variety of materials with low melting temperatures can be safely incorporated. Also discussed is the potential of carbon nanofibers as an improved method of polymer reinforcement by tailoring morphology through reaction parameters.

The use of carbon nanofibers for advanced materials and technologies has been gaining momentum. This work has helped to show the viability of these structures for use in the near future. Although other technologies with superior properties (i.e. carbon nanotubes) tend to be more widely studied, the ability to cheaply and simply produce carbon nanofibers by catalysis is an attractive motivator to shift the paradigm.

7 References

1. Maynard AD. *Nanotechnology: The next big thing, or much ado about nothing?* The Annals of Occupational Hygeine 2007;51(1):1-12.
2. Iijima S. *Helical microtubules of graphitic carbon*. Nature 1991;354(6348):56-58.
3. Iijima S, Ichihashi T. *Single-shell carbon nanotubes of 1-nm diameter*. Nature 1993;363(6430):603-05.
4. Bethune DS, Klang CH, deVries MS, Gorman G, Savoy R, Vasquez J, et al. *Cobalt catalysed growth of carbon nanotubes with single atomic layer walls*. Nature 1993;363(6430):605-07.
5. (Ed.) MJOC. Carbon Nanotubes: Properties and Applications. Boca Raton, FL: CRC Press; 2006.
6. Serp P, Corrias M, Kalck P. *Carbon nanotubes and nanofibers in catalysis*. Applied Catalysis A: General 2003;253(2):337–35.
7. Geim AK, Novoselov KS. *The rise of graphene*. Nature Materials 2007;6(3):183-91.
8. Efremenko I. *Implication of palladium geometric and electronic structures to hydrogen activation on bulk surfaces and clusters*. Journal of Molecular Catalysis A: Chemical 2001;173(1-2):19-59.
9. Phillips J, Shiina T, Nemer M, Lester K. *Graphitic structures by design*. Langmuir 2006;22(23):9694-703.
10. Wu NL, Phillips J. *Carbon deposition on platinum during ethylene oxidation*. Journal of Catalysis 1988;113(2):383-97.
11. Rodriguez NM, Chambers A, Baker RTK. *Catalytic engineering of carbon nanostructures*. Langmuir 1995;11(10):3862-66.
12. Anderson PE, Rodriguez NM. *Influence of the support on the structural characteristics of carbon nanofibers produced from the metal-catalyzed decomposition of ethylene*. Chemistry of Materials 2000;12(3):823-30.
13. Park C, Baker RTK. *Carbon deposition on iron-nickel during interaction with ethylene-hydrogen mixtures*. Journal of Catalysis 1998;179(2):361-74.

14. Chambers A, Rodriguez NM, Baker RTK. *Modification of the catalytic behavior of cobalt by the addition of copper*. Journal of Physical Chemistry 1995;99(26):10581–89.
15. Owens WT, Rodriguez NM, Baker RTK. *Carbon filament growth on platinum catalysts*. Journal of Physical Chemistry 1992;96(12):5048-53.
16. Wu NL, Phillips J. *Catalytic etching of platinum during ethylene oxidation*. Journal of Physical Chemistry 1985;89(4):591–600.
17. Baker RTK, Barber MA, Harris PS, Feates FS, Waite RJ. *Nucleation and growth of carbon deposits from the nickel catalyzed decomposition of acetylene*. Journal of Catalysis 1972;26(1):51-62.
18. Rodriguez NM. *A review of catlytically grown carbon nanofibers*. Journal of Materials Research 1993;8(12):3233-50.
19. Kock AJHM, Bokx PKd, Boellaard E, Klop W, Geus JW. *The formation of filamentous carbon on iron and nickel catalysts*. Journal of Catalysis 1985;96(2):468-80.
20. Yang RT, Chen JP. *Mechanism of carbon filament growth on metal catalysts*. Journal of Catalysis 1989;115(1):52-64.
21. Tibbetts GG, Devoura MG, Roddaa EJ. *An adsorption-diffusion isotherm and its application to the growth of carbon filaments on iron catalyst particles*. Carbon 1987;25(3):367-75.
22. Hughes TV, Chambers CR, inventors. Manufacture of Carbon Filaments. US patent 405480. 1889.
23. Ruston WR, Warzee M, Hennaut J, Waty J. *The solid reaction products of the catalytic decomposition of carbon monoxide on iron at 550°C*. Carbon 1969;7(1):47-50.
24. Robertson SD. *Carbon formation from methane pyrolysis over some transition metal surfaces - I. Nature and properties of the carbons formed*. Carbon 1970;8(3):365-74.
25. Baird T, Fryer JR, Grant B. *Structure of filamentous carbon*. Nature 1971;233(5318):329-30.

26. Rostrup-Nielsen J, Trimm DL. *Mechanisms of carbon formation on nickel-containing catalysts*. Journal of Catalysis 1977;48(1-3):155-65.
27. Bokx PKd, Kock AJHM, Boellaard E, Klop W, Geus JW. *The formation of filamentous carbon on iron and nickel catalysts - I thermodynamics*. Journal of Catalysis 1985;96(2):454-67.
28. Boellaard E, Bokx PKd, Kock AJHM, Geus JW. *The formation of filamentous carbon on iron and nickel catalysts - III morphology*. Journal of Catalysis 1985;96(2):481-90.
29. Park C, Rodriguez NM, Baker RTK. *Carbon deposition on iron-nickel during interaction with carbon monoxide-hydrogen mixtures*. Journal of Catalysis 1997;169(1):212-27.
30. Park C, Baker RTK. *Carbon deposition on iron-nickel during interaction with ethylene-carbon monoxide-hydrogen mixtures*. Journal of Catalysis 2000;190(1):104-17.
31. Merkulov VI, Lowndes DH, Wei YY, Eres G, Voelkl E. *Patterned growth of individual and multiple vertically aligned carbon nanofibers*. Applied Physics Letters 2000;76(24):3555-57.
32. Lee JL, Lee TJ, Park J. *Carbon nanofibers grown on sodalime glass at 500°C using thermal chemical vapor deposition*. Chemical Physics Letters 2001;340(5):413-18.
33. Rodriguez NM, Kim MS, Baker RTK. *Deactivation of copper-nickel catalysts due to changes in surface composition*. Journal of Catalysis 2003;140(1):16-29.
34. Terrones H, Hayashi T, Munoz-Navia M, Terrones M, Kim YA, Grobert N, et al. *Graphitic cones in palladium catalysed carbon nanofibers*. Chemical Physics Letters 2001;343(3-4):241-50.
35. Lupu D, Radu-Biris A, Misan I, Jianu A, Holzhuter G, Burkel E. *Hydrogen uptake by carbon nanofibers catalyzed by palladium.* International Journal of Hydrogen Energy 2004;29(1):97-102.
36. Ngo Q, Cassell AM, Radmilovic V, Li J, Krishnan S, Meyyappan M, et al. *Palladium catalyzed formation of carbon nanofibers by plasma enhanced chemical vapor deposition*. Carbon 2007;45(2):424-8.

37. Vajtai R, Kordas K, Wei BQ, Bekesi J, Leppavuori S, George TF, et al. *Carbon nanotube network growth on palladium seeds*. Materials Science and Engineering: C 2002;19(1):271-74.

38. Wu X, Gallego NC, Contescu CI, Tekinalp H, Bhat VV, Baker FS, et al. *The effect of processing conditions on microstructure of Pd-containing activated carbon fibers*. Carbon 2008;46(1):54-61.

39. Breton Y, Verstraete M, Fleurier R, Cacciaguerra T, Charlier J-C, Thomann A-L, et al. *Anomalous ESR behavior of carbon nanofilaments grown from palladium seeds*. Carbon 2004;42(5):1049-52.

40. Arrhenius S. *On the Rate of Reaction of the Inversion of Sucrose by Acids*. Zeitschrift fuer physikalische Chemie 1889;4:226-48.

41. deJong KP, Geus JW. *Carbon nanofiber: synthesis and applications*. Catalysis Reviews - Science and Engineering 2000;42(4):481-510.

42. Atwater MA, Phillips J, Leseman ZC. *Controlling carbon nanofibres morphology for improved composite reinforcement*. International Journal of Materials and Structural Integrity 20XX;In Press.

43. Knight DS, White WB. *Characterization of diamond films by Raman spectroscopy*. Journal of Materials Research 1989;4(2):385-93.

44. Doorn SK, Zheng L, O'Connell MJ, Zhu Y, Huang S, Liu J. *Raman spectroscopy and imaging of ultralong carbon nanotubes*. Journal of Physical Chemistry: B 2005;109(9):3751-58.

45. Dillon AC, Parilla PA, Alleman JL, Gennett T, Jones KM, Heben MJ. *Systematic inclusion of defects in pure carbon single-wall nanotubes and their effect on the Raman D-band*. Chemical Physics Letters 2005;401(4-6):522-28.

46. Baker RTK, Harris PS, Terry S. *Unique form of filamentous carbon* Nature 1975;253(5486):37-39.

47. Mackin TJ, Warren PD, Evans AG. *Effect of fiber roughness on interface sliding in composites*. Acta Metallurgica et Materialia 1992;40(6):1251-57.

48. Endo M, Kim YA, Hayashi T, Yanagisawa T, Muramatsu H, Ezaka M, et al. *Microstructural changes induced in ‘’stacked cup’’ carbon nanofibers by heat treatment.* Carbon 2003;41(10):1941-47.

49. Taylor HS, Hil DG. *The reactions of ethylene hydrogen and the saturated hydrocarbons under the Influence of excited mercury*. Journal of the American Chemical Society 1929;51(10):2922–36.

50. Turkevich J, Kim G. *Palladium: preparation and catalytic properties of particles of uniform size* Science 1970;169(3948):873 - 79.

51. Weigle JC, Phillips J. *Novel dual-bed reactors: utilization of hydrogen spillover in reactor design*. Langmuir 2004;20(4):1189–93.

52. Weigle JC, Phillips J. *Modeling hydrogen spillover in dual-bed catalytic reactors*. American Institute of Chemical Engineers 2004;50(4):821 - 28.

53. Menéndez JA, Radovic LR, Xia B, Phillips J. *Low-temperature generation of basic carbon surfaces by hydrogen spillover*. Journal of Physical Chemistry 1996;100(43):17243–48.

54. Westbrook CK, Dryer FL, Schug KP. A comprehensive mechanism for the pyrolysis and oxidation of ethylene. Paper presented at: Symposium (International) on Combustion, 19th, 1982.

55. Halstead MP, Leathard DA, Marshall RM, Purnell JH. *The reaction of hydrogen atoms with ethylene*. Proceedings of the Royal Society: A 1970;316(1527): 575-91.

56. Yoon YJ, Baik HK. *Catalytic growth mechanism of carbon nanofibers through chemical vapor deposition*. Diamond and Related Materials 2001;10(3-7):1214-17.

57. Flanagan TB, Oates WA. *The palladium-hydrogen system*. Annual Review of Materials Research 1991;21:269-304.

58. Xu Y-Q, Flor E, Schmidt H, Smalley RE, Hauge RH. *Effects of atomic hydrogen and active carbon species in 1 mm vertically aligned single-walled carbon nanotube growth*. Applied Physics Letters 2006;89(12):123116.

59. Davis SM, Zaera F, Somorjai GA. *The reactivity and composition of strongly adsorbed carbonaceous deposits on platinum. Model of the working hydrocarbon conversion catalyst*. Journal of Catalysis 1982;77(2):439-59.

60. Webb G. *The formation and role of carbonaceous residues in metal-catalyzed reactions of hydrocarbons*. Catalysis Today 1990;7(2):139-55.

61. Frenklach M, Ping J. *On the role of surface migration in the growth and structure of graphene layers*. Carbon 2004;42(7):1209-12.
62. Frenklach M, Ramachandra MK, Matula RA. Soot formation in shock-tube oxidation of hydrocarbons. Paper presented at: 20th Symposium on Combustion, 1984.
63. Wei T-C, Phillips J. Thermal and catalytic etching mechanisms of metal catalyst reconstruction. Advances in Catalysis. New York: Academic Press; 1996. p. pp. 359-421.
64. Atwater MA, Phillips J, Doorn SK, Luhrs CC, Fernandez Y, Menendez JA, et al. *The production of carbon nanofibers and thin films on palladium catalysts from ethylene–oxygen mixtures*. Carbon 2009;47(9):2269–80.
65. Luhrs CC, Garcia D, Terani M, Al-Haik M, Taha MR, Phillips J. *Generation of carbon nanofilaments on carbon fibers at moderate temperatures*. Carbon 20XX;In Press.
66. Zhu Z, Lu Y, Qiao D, Bai S, Hu T, Li L, et al. *Self-catalytic behavior of carbon nanotubes*. Journal of the American Chemical Society 2005;127(45):15698-99.
67. Venkateswaran R, Black MH, Scacchi G. *The dual nature of carbon: catalyst and inhibitor*. Carbon 1994;32(5):911-19.
68. Jr. BWR, inventor. Process for making carbon fiber. US patent 3,764,662. 1973.
69. Harris PJF. *Carbon nanotube composites*. International Materials Reviews 2004;49(1):31-43.
70. Hammel E, Tang X, Trampert M, Schmitt T, Mauthner K, Eder A, et al. *Carbon nanofibers for composite applications*. Carbon 2004;42(5-6):1153-58.
71. Downs WB, Baker RTK. *Modification of the surface properties of carbon fibers via the catalytic growth of carbon nanofibers*. Journal of Materials Research 1995;10(3):625-33.
72. Lin Y, Zhou B, Fernando KAS, Liu P, Allard LF, Sun Y-P. *Polymeric Carbon Nanocomposites from carbon nanotubes functionalized with matrix polymer*. Macromolecules 2003;36(19):7199-204.

73. Shi D, Lian J, He P, Wang LM, Xiao F, Yang L, et al. *Plasma coating of carbon nanofibers for enhanced dispersion and interfacial bonding in polymer composites*. Applied Physics Letters 2003;83(25):5301-03.
74. Ford WD, inventor. Method of making cellular refractory thermal insulating material. US patent 3,121,050. 1964.
75. Mitchell CV, inventor. Carbon Foam. US patent 3,302,999. 1967.
76. Knippenberg WF, Lersmacher B. *Carbon foam*. Phillips Technical Review 1976;36(4):93-103.
77. Inagaki M, Morishita T, Kuno A, Kito T, Hirano M, Suwa T, et al. *Carbon foams prepared from polyimide using urethane foam template*. Carbon 2004;42(3):497-502.
78. Chen Y, Chen B-Z, Shi X-C, Xu H, Hu Y-J, Yuan Y, et al. *Preparation of pitch-based carbon foam using polyurethane foam template*. Carbon 2007;45(10):2132-34.
79. Lee J, Sohn K, Hyeon T. *Fabrication of novel mesocelluler carbon foams with uniform ultralarge mesopores*. Journal of the American Chemical Society 2001;123(21):5146-47.
80. Lee J, Han S, Hyeon T. *Synthesis of new nanoporous carbon materials using nanostructured silica materials as templates*. Journal of Materials Chemistry 2004;14(4):478-86.
81. Klett JW, McMillan AD, Gallego NC, Walls CA. *The role of structure on the thermal properties of graphitic foams*. Journal of Materials Science 2004;39(11):3659-76.
82. Li T-Q, Wang C-Y, An B-X, Wang H. *Preparation of graphitic carbon foam using size-restriction method under atmospheric pressure*. Carbon 2005;43(9):2030-32.
83. Wang M-X, Wang C-Y, Zhang X-L, Zhang W. *Effects of the stabilization conditions of the structural properties of mesophase-pitch-based carbon foams*. Carbon 2006;44(15):3371-72.
84. Wang X, Zhong J, Wang Y, Yu M, Wang Y. *The study on the formation of graphitic foam*. Materials Letters 2007;61(3):741-46.

85. Wang M-X, Wang C-Y, Li T-Q, Hu Z-J. *Preparation of mesophase-pitch-based carbon foams at low pressures*. Carbon 2008;46(1):84-91.
86. Gallego NC, Klett JW. *Carbon foams for thermal management*. Carbon 2003;41(7):1461-66.
87. Knox JH, Gilbert MT, inventors. Preparation of porous carbon. US patent 4,263,268. 1981.
88. Klett JW, inventor. Process for making carbon foam. US patent 6,033,506. 2000.
89. Bennett B, Stiller A, inventors. Method of making carbon foam at low pressure. US patent US 6,797,251 B1. 2004.
90. Stiller AH, Stansberry PG, Zondlo JW, inventors. US patent 5,888,469. 1999.
91. Smith HA. *Catalysis of the Formation of Urethanes*. Journal of Applied Polymer Science 1963;7(1):85-95.
92. Gloskey CR, inventor. Process for the preparation of urethane foam. US patent 4,532,262. 1985.
93. Qi X, Ruan X, Pan C. *Graphitization of solid carbon nanofibers at an unexpectedly low temperature*. Materials Letters 2007;61(21):4272-75.
94. Ajayan P, Carrillo A, Chakrapani N, Kane RS, Wei B, inventors. Carbon nanotube foam and method of making and using thereof. US patent US 2006/0073089 A1. 2006.
95. Wang J, inventor. Porous carbon foam composites, applications and processes of making. US patent 20090136809. 2009.
96. Klett JW, inventor. Pitch-based carbon foam and composites. US patent US 6,387,343 B1. 2002.